UNIVERSITI PUTRA MALAYSIA

FIRST-PRINCIPLES STUDY OF CARBON MONOXIDE ADSORPTION ON SILICENE MONOLAYER

EZZRIN IZZATI BINTI JAMALUDDIN

UNIVERSITI PUTRA MALAYSIA

BERILMU BERBAKTI

FIRST-PRINCIPLES STUDY OF CARBON MONOXIDE ADSORPTION ON SILICENE MONOLAYER

By

EZZRIN IZZATI BINTI JAMALUDDIN

Thesis submitted to the School of Graduate Studies, Universiti Putra Malaysia, in Fulfilment of the Requirements for the Bachelor of Science in Physics with Honours

DEDICATIONS

I humbly dedicate this piece of work to my loving parents, Mr Jamaluddin Awang Nong and Mrs Shamsida Abdan, for their ultimate support and love, to my supervisor, Dr. Chan Kar Tim, for his endless guidance and teaching, and to my friends for their encouragement and pieces of advice.

Thank you for all of the support and guidance throughout the process.

Abstract of thesis presented to the Senate of Universiti Putra Malaysia in fulfilment of the requirement for the Bachelor of Science in Physics with Honours

First-Principles Study on Carbon Monoxide Adsorption on Silicene Monolayer

By

EZZRIN IZZATI BINTI JAMALUDDIN

195911

Supervisor: Dr. Chan Kar Tim

Department: Department of Physics, Faculty of Science

Silicene, has shown to have significant properties in many studies and applications. Many people has shown keen interest to be able to understand precisely on how are these properties such as structural and electronic properties are affected by adsorbing carbon monoxide onto silicene sheet.

The silicene system with adsorbed carbon monoxide was studied using first principles analysis based on density functional theory in this work. Quantum ESPRESSO was used in conjunction with the local-density approximation to perform the calculations. Other softwares were installed and used in this research, including Xcrysden and Gnuplot. Quantum ESPRESSO has been used to simulate the structure of silicene sheets, and the findings have demonstrated to be similar to the experimental data, proving that it is an appropriate and valid quantum simulation software. Results that have been obtained

from simulated silicene monolayer adsorbed with carbon monoxide have shown that carbon monoxide has the tendency to be at its most stable configuration at hollow site of silicene sheet. As for the electronic properties, after the density of state and electronic band structure have been studied, we observed that the band structure of the silicene system after being adsorbed with carbon monoxide has been shifted where the gap between the band gap is widen. The calculated value of E_{ad} is -0.0902414251 eV / atom. Due to the small adsorption energy value, there is little interactions between CO and silicene monolayer. Therefore, CO is physisorbed on silicene via Van der Waals interactions. In addition, the distance between the position to place CO on silicene sheet is fixed at 2.5 Å while the distance between carbon and oxygen atom is set at 1.128 Å.

Abstrak tesis yang dikemukakan kepada Senat Universiti Putra Malaysia sebagai memenuhi keperluan untuk Bacelor Sains Fizik dengan Kepujian

Kajian Prinsip Pertama Mengenai Pengjerapan Karbon Monoksida Pada Lapisan Tunggal Silisin

Oleh

EZZRIN IZZATI BINTI JAMALUDDIN

195911

Penyelia: Dr. Chan Kar Tim

Jabatan: Jabatan Fizik, Fakulti Sains

Silisin, telah terbukti mempunyai sifat penting dalam pelbagai kajian dan aplikasi. Ramai orang telah menunjukkan minat yang mendalam untuk dapat memahami dengan lebih tepat bagaimana sifat-sifat seperti sifat struktur dan elektronik boleh dipengaruhi dengan pengjerapan karbon monoksida ke dalam lembaran silisin.

Sistem silisin yang telah dijerap dengan karbon monoksida telah dikaji menggunakan analisis prinsip pertama berdasarkan teori fungsi ketumpatan dalam penyelidikan ini. Quantum ESPRESSO digunakan bersama dengan penghampiran kepadatan tempatan untuk melakukan pengiraan. Perisian lain dipasang dan digunakan dalam penyelidikan ini, termasuk Xcrysden dan Gnuplot. Quantum ESPRESSO telah digunakan untuk mensimulasikan struktur lembaran silisin, dan penemuan tersebut terbukti serupa dengan data eksperimen, membuktikan bahawa ia adalah perisian simulasi kuantum yang sesuai dan sah. Hasil yang diperoleh dari simulasi lembaran tunggal silisin yang diserap

dengan karbon monoksida telah menunjukkan bahawa karbon monoksida mempunyai kecenderungan untuk berada pada konfigurasi yang paling stabil di lokasi lembaran silisin berongga. Bagi sifat elektronik, setelah kepadatan struktur jalur keadaan dan elektronik telah dikaji, kami melihat bahawa struktur jalur sistem silisin setelah diserap dengan karbon monoksida telah dialihkan di mana jurang antara jurang jalur semakin luas. Nilai tenaga penjerapan, E_{ad} yang dikira ialah -0.0902414251 eV / atom. Oleh kerana nilai tenaga penjerapan kecil, terdapat sedikit interaksi antara karbon monosikda dan lembaran tunggal silisin. Oleh itu, karbon monosikda telah diserap secara fizik pada silisin melalui interaksi *Van der Waals*. Di samping itu, jarak antara kedudukan untuk meletakkan karbon monosikda pada lembaran silisin ditetapkan pada 2.5 Å sementara jarak antara atom karbon dan oksigen ditetapkan pada 1.128 Å.

ACKNOWLEDGEMENTS

First and foremost, praises and thanks to God, the Almighty, for His showers of blessings throughout my research process and work to complete this thesis successfully.

I would like to express my deep and sincere gratitude to my research supervisor, Dr. Chan Kar Tim, Senior Lecturer in the Department of Physics at Universiti Putra Malaysia, for giving me the opportunity to do this research and providing me invaluable guidance throughout the research process. His enthusiasm, vision, sincerity and motivation has deeply inspired me. He has taught me the methodology in detail for me to carry out the research and to present the work as clearly as possible. It was indeed a great privilege and such an honour to work and study under his supervision and guidance. I am extremely grateful for what he has offered me. I would also like to thank him for his kindness, patience and empathy. I could not have imagined having a better advisor and mentor for my thesis research.

I am extremely and utterly grateful for both of my parents, Mr. Jamaluddin and Mrs. Shamsida for having me as their daughter and supporting me throughout my life. I am extending my heartfelt thanks for their endless and ultimate love, prayers, teachings and sacrifices for educating and preparing me for my future. They are truly my greatest motivation and supporters. To my one and only sister, Arissa, who is also constantly showing me your support, I truly appreciate your words of encouragement and pieces of advice.

Last but not least, I would like to express my gratitude and thanks to all of my friends, especially to my fellow final year project partners, Haiqal and Akmal for the keen interest shown to complete the thesis successfully. I appreciate and am grateful to them for the stimulating discussions, for the sleepless nights when we were working together catching up the deadlines and for all of the fun we have had in our degree years. Thank you so much.

TABLE OF CONTENTS

	Page
DEDICATIONS	I
ABSTRACT	II
ABSTRAK	IV
ACKNOWLEDGEMENTS	VI
APPROVAL	VIII
DECLARATION	IX
LIST OF TABLES	XII
LIST OF FIGURES	XIII
LIST OF ABBREVIATIONS	XV
CHAPTER	
1 **INTRODUCTION**	1
1.1 Introduction to Silicene	1
1.1.1 Stability of Low-Buckled Structure of Silicene	2
1.1.2 Application of Silicene in Nanoelectronics	5
1.2 Introduction to Poisonous Gas	6
1.3 Gas Sensing Using Different Materials	8
1.4 Problem Statement	10
1.5 Objectives	10
2 **LITERATURE REVIEW**	11
2.1 Properties of Silicene	11
2.1.1 Structure of Silicene	11
2.1.2 Electronic Properties of Silicene	16
2.2 Gas Molecules Adsorption on Silicene	18
2.3 Density Functional Theory	22
2.4 Quantum ESPRESSO	26
3 **METHODOLOGY**	29
3.1 Installation of Quantum ESPRESSO	29
3.2 Material Modelling Using VESTA	32
3.2.1 Building Unit Cell using VESTA	32
3.2.2 Building Super Cell of Silicene	34
3.2.3 Modelling CO Molecule	35
3.2.4 Modelling of Adsorbed CO on Silicene	36
3.3 Quantum Simulation on Silicene	37
3.3.1 Input and Output File for QE Calculation	37
3.3.2 Determination of Kinetic Energy Cutoff and K-Points	43

3.3.3 Relaxation, Self Consistent Field and Non-Self Consistent Field 44
3.3.4 Computation of Ground State Energy 48
3.3.5 Density Of States Calculation 49
3.3.6 Band Structure Calculation 51

4 **RESULTS AND DISCUSSION** 54
4.1 Silicene Sheet Modelling 54
4.2 Convergence Test of Kinetic Energy Cutoff and K-points 56
4.3 Structural and Electronic Properties of Silicene Sheet 58
4.4 Structural Stabilities of CO on Silicene System 61
4.5 Electronic Properties of Silicene Sheet Adsorbed with Carbon Monoxide 62

5 **CONCLUSION** 65
5.1 Conclusion 65
5.2 Future Works 66

REFERENCES 67
APPENDICES 70

LIST OF TABLES

Table		Page
2.1	Structural parameters of silicene compared to graphene and germanene	14
2.2	A table of adsorption energy (E_{ad}), charge transfer (δq), binding distance (d) and band gap (E_g)	21
2.3	A summary of basic computations that can be performed	28
4.1	The convergence of total energy with respect to the kinetic energy cutoff where 1 Rydberg (Ry) is equals to 13.606 eV	56
4.2	The convergence of total energy with respect to the k-points where 1 Rydberg (Ry) is equals to 13.606 eV	57
4.3	Final output of simulation result with respect to the position of the silicon atom in silicene sheet	59
4.4	The simulation output of CO adsorbed on silicene at four different sites with four different orientations each	61

LIST OF FIGURES

Figure		Page
1.1	This is the top view and side view of the silicene lattice. The black rhombus represents a primitive cell. The buckled height is shown in the side view and denoted as *h*	2
1.2	The visualization of buckled structure of silicene	3
1.3	The graph of binding energy versus hexagonal lattice constant of silicene and germanene. The black and dashed green curves represent the phonon dispersion curves calculated using force-constant and linear response theory, respectively	4
1.4	This figure shows what will happen to human body when there is a consumption of CO	7
1.5	The burning of fossil fuel by factories	8
2.1	The visualization of a) crystal structure of silicene, the dashed lines indicate the unit cell and the basis is made up of two Si atoms, denoted by A and B, while b) the illustration of sp_2 hybridization in silicon	12
2.2	The visualization of (i) the planar silicene, (ii) simply buckled silicene, (iii) buckled silicene with a ($\sqrt{3}\times\sqrt{3}$) unit cell and (iv) buckled silicene with a (4×4) unit cell. The buckling distance is denoted as *d*. Both top and side views are presented. Shadow regions presented the unit cells	15
2.3	The illustrations of all possible adsorption sites on silicene	16
2.4	The illustration of the band structures of graphene, silicene, and germanene, respectively	18
2.5	The illustration of the most stable configuration for the two same adsorbates as mentioned in Table 2.2, (a) C–Si distance is 4.02 Å while (b) the distance of the newly formed N–Si bond is 2.10 Å	21
3.1	The main interface of VESTA	32
3.2	Visualization of unit cell structure	33
3.3	Illustration of the view along the a axis	33
3.4	Visualization of unit cell for silicene monolayer a) with some symmetry atoms , while b) the exact unit cell with only two atoms	34
3.5	Illustration of silicene super cell	35
3.6	The visualization of complete 3×3 monolayer silicene	35
3.7	The visualization of CO molecule model	36
3.8	Illustration of modelling of CO molecules in 3×3 silicene	36

3.9	Relaxation calculation input file of silicene	38
3.10	Self-Consistent Field calculation input file of silicene	39
3.11	Calculation flow chart	44
3.12	The command for relaxation calculation	45
3.13	The command of scf calculation	45
3.14	Input file of nscf calculation	47
3.15	Coordinates when silicene is adsorbed with CO	49
3.16	The command for DOS input file	49
3.17	The commands for DOS plotting in Gnuplot	50
3.18	The command for pDOS input file	51
3.19	The input file of bands	52
3.20	The command for bands_pp input file	53
3.21	The input file of run.py	53
4.1	The (3×3) pristine silicene sheet and CO adsorbed silicene sheet	55
4.2	The convergence of total energy with respect to the k-points where 1 Rydberg (Ry) is equals to 13.606 eV	57
4.3	The graph of total energy versus k-points	58
4.4	The density of states (DOS) and electronic band structure of pristine silicene sheet	60
4.5	The density of state of adsorbed CO on silicene sheet	63
4.6	The electronic band structure of the adsorbed CO on silicene sheet	63

LIST OF ABBREVIATIONS

DFT	Density Functional Theory
PW	Plane Wave
PP	Pseudopotentials
PWGUI	Plane wave graphic user interface
scf	self-consistent calculation
CO	Carbon Monoxide
DOS	Density of States
Ry	Rydberg
LDA	Local-Density Approximation

CHAPTER 1

INTRODUCTION

1.1 Introduction to Silicene

Silicene is a two-dimensional allotrope of silicon that has a wide range of chemical and physical properties that are expected to be helpful (Spencer and Morishita, 2018). Silicene is the silicon-based analogue of graphene and it is a novel crystalline silicon form (Yan Voon and Guzmán-Verri, 2014). This graphene equivalent has gotten a lot of attention in recent years. Silicene is monoatomic because it is made up entirely of silicon atoms and has a single silicon atomic layer (Zhuang et al., 2015). Unlike graphene and other 2D materials, however, silicene is not perfectly planar. It has a buckled honeycomb surface instead. In particular, silicene demonstrates photoelectronic effects, lower thermal conductivity, and greater chemical activity than bulk silicon materials since it is a one-atom thick silicon sheet structured in a honeycomb lattice (Zhao et al., 2016). The existence of silicene is very interesting because it can be considered quite similar to graphene as it is two-dimensional and has a Dirac cone, a surface in materials that has unique electron transport.

As the three-dimensional shape of silicene is a diamond lattice, silicene is harder to make compared to graphene as it can only be created through epitaxial growth rather than exfoliation. However, silicene still appear to have a range of interesting features. For one point, the interactions between the layers in multi-layered silicene are extremely

strong, far stronger than the individual layers in multi-layered graphene. There are oxygenated forms of silicene called two-dimensional silica, as well as silicene nanoribbons, in addition to pure silicene (Jeevanandam et al., 2018).

1.1.1 Stability of Low-Buckled Structure of Silicene

Silicene, unlike graphene, is not a perfectly flat sheet. In comparison to graphene, which has a planar geometry, silicene has a buckled structure. Figure 1.1 depicts the atomic structure of silicene, which features a low-buckled honeycomb lattice. Figure 1.2 illustrates the buckled structure of silicene.

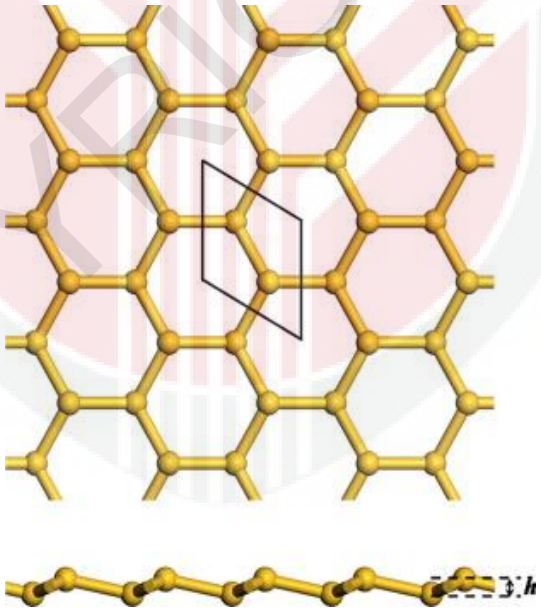

Figure 1.1: This is the top view and side view of the silicene lattice. The black rhombus represents a primitive cell. The buckled height is shown in the side view and denoted as *h* (Zhao et al., 2016).

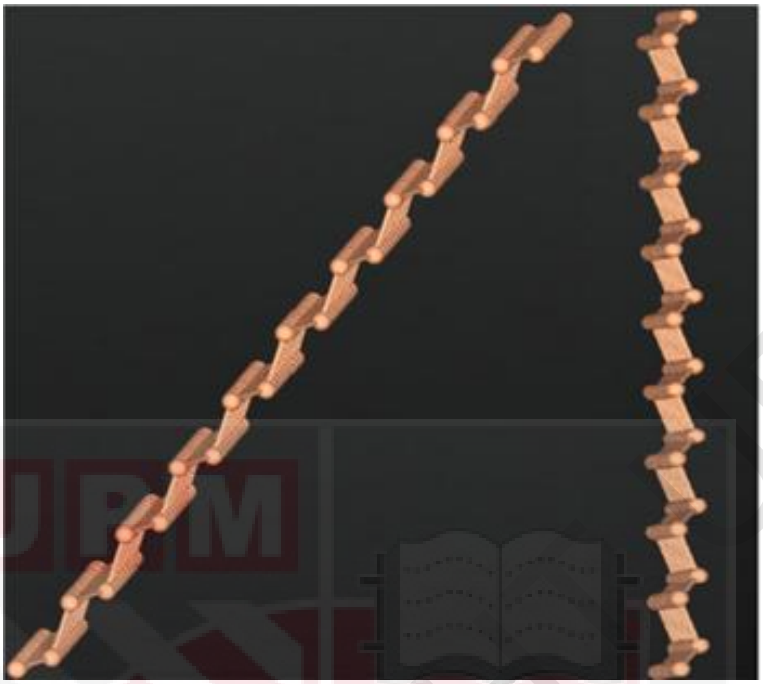

Figure 1.2: The visualization of buckled structure of silicene (Kharadi et al., 2020).

In research from Zhao et al. (2016), they reported that the binding energy curves show local minima for planar, low-buckled, and high-buckled honeycomb structures. In a huge portion of the Brillouin zone, planar honeycomb structures exhibit imaginary phonon frequencies and have greater energy than their low-buckled and high-buckled counterparts. As a result, planar formations in silicene are unstable. Meanwhile, imaginary phonon frequencies can be found in Si high-buckled honeycomb structures with a buckling height of about 2Å. On the (2 × 2) supercell, further optimization of the high-buckled structure leads to an instability with a gathering tendency. Figure 1.3 shows binding energy versus hexagonal lattice constant of silicene and germanene, and the black and dashed green curves are phonon dispersion curves calculated using force-constant and linear response theory, respectively.

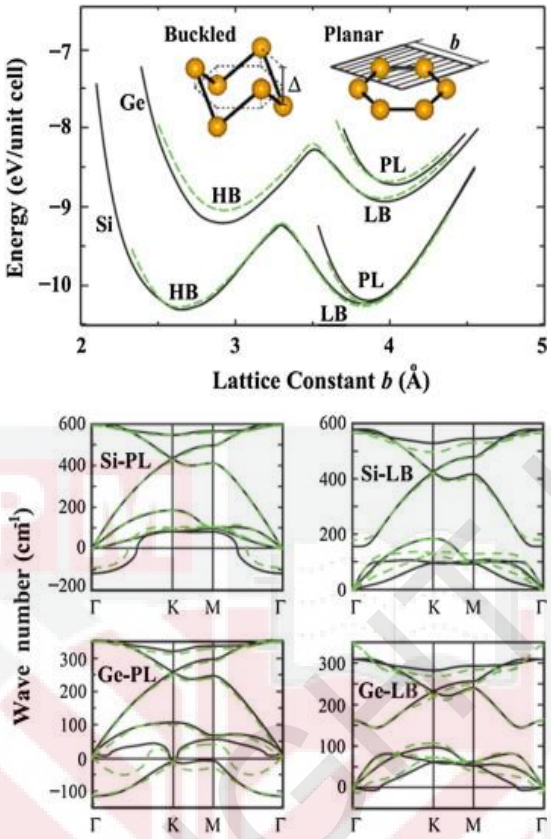

Figure 1.3: The graph of binding energy versus hexagonal lattice constant of silicene and germanene. The black and dashed green curves represent the phonon dispersion curves calculated using force-constant and linear response theory, respectively (Zhao et al., 2016).

As a result, the high-buckled structures for Si do not correlate to actual Born–Oppenheimer surface local minima. Low-buckled structures for Si, on the other hand, have positive phonon dispersion curve values across the Brillouin zone and are hence dynamically stable (Zhao et al., 2016). For the low-buckled structures, the calculated Si–Si bond lengths are around 2.2–2.4Å. Since it should yield both a band gap and polarised spin-states that may be controlled with a perpendicular electrical field, this buckling gives silicene an advantage over graphene (Drummond et al., 2012). Previous

density functional theory (DFT) studies have indicated that this low buckled form is the most stable (Zhao et al., 2016).

1.1.2 Application of Silicene in Nanoelectronics

Silicene is unlike graphene as it possesses a band gap, nanoscale semiconductors with a wide range of uses, such as light emitting diodes and computer processors, will be possible to build. It is easier to open and tune the bandgap of silicene than graphene with a planar structure because of the buckling development (Raya et al., 2021). These properties make silicene appealing for use in nanoelectronics. Due to its unique features, silicene has shown promise in a variety of technical applications, including field-effect transistors, spintronic and valleytronic devices, thermoelectric devices, chemical sensors, hydrogen storage, and as an electrode material in Li batteries (Raya et al., 2021).

The band gap in silicene may be opened without affecting carrier mobility, making it excellent for fabricating high-performance Field-Effect Transistor (FET) devices. Gablech et al. (2018) stated that previous study has calculated silicene sensitivity and selectivity on detection of NO, NO_2, NH_3, and CO gases using density functional theory (DFT) and the no-equilibrium Green's function approach. Calculations using density functional theory have revealed that silicene clusters will be ideal for FET and nanoelectronics applications.

1.2 What is Poisonous Gas?

In this era of globalization that is full of swift evolution in technologies and fast development in industries, people live their lives in a better and splendour way. However, this magnificent evolution leads to a higher consumption of toxic substances and harmful gases. The consumption of these poisonous gases does nothing good to the human population. In fact, the pollution of the Earth has increased for the past decades and humans are all exposed to small quantities of toxic gases even on a daily basis. The deliberate discharge of chemical warfare weapons, the release of hazardous industrial gas, and the products of chemical or combustion processes are all examples of manmade harmful pollutants that have been released into the atmosphere (Lambrini et al., 2018).

Some of the most frequent dangerous substances are NO, NO_2, SO, SO_2, CO, NH_3, nitrogen-containing compounds, sulfur-containing compounds, hydrocarbons and volatile organic compounds. Anthropogenic gases are the primary sources of these gases (Barea et al., 2014).

One of the most common harmful gases on the planet is carbon monoxide. It's colourless and odourless. CO is a toxic gas that is produced when incomplete combustion occurs. Car exhaust emissions are particularly important, as carbon monoxide levels in confined parking lots can reach dangerous levels. The primary sources of human exposure to this chemical are tobacco smoke and heavy traffic. CO can cause heart and pulmonary diseases, behavioural disturbances, central nervous system involvement, movement and

vision difficulties, headache, weariness, coma, dyspnea, and even death, depending on its concentration in the air. People are almost all exposed to it in some way, but it frequently results in catastrophe, earning it the moniker "silent killer". Figure 1.4 shows what happens to the human body when a person inhales CO.

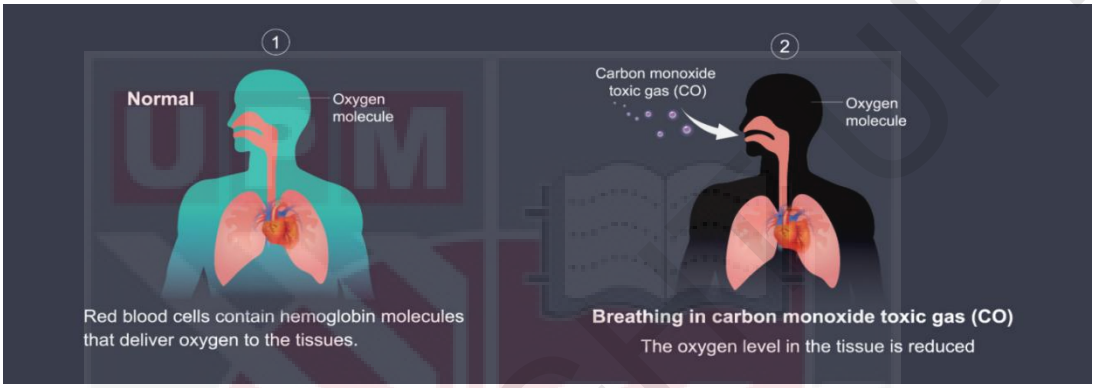

Figure 1.4: This figure shows what will happen to human body when there is a consumption of CO.

Carbon dioxide (CO_2) is a colourless, odourless, and tasteless gas. It is also one of the greenhouse gases (Lambrini et al., 2018). Carbon dioxide is naturally found in groundwater, rivers and lakes, ice caps, glaciers, and ocean since it is soluble in water (Rumbeiha and Oehme, 2005). It can be found in petroleum and natural gas reserves. At normal concentrations, carbon dioxide has no odour; nevertheless, at high concentrations, it produces a harsh and acidic stench. CO_2 is a gas that is slightly poisonous. A person can only suffer from headaches, anxiety, emesis, dizziness, and other symptoms by inhaling carbon dioxide for an extended period of time.

Nitrogen monoxide (NO) is another major hazardous gas. Human activity, mostly the burning of fossil fuels, is the primary source of NO. Photochemical smog, acid rain,

ozone depletion, and greenhouse effects are all possible consequences of excessive NO levels in the atmosphere (Kakaei et al., 2019). Figure 1.5 shows the burning of fossil fuel by factories.

Figure 1.5: The burning of fossil fuel by factories

1.3 Gas Sensing Using Different Materials

In research from Jeevanandam et al. (2018), the past century saw a massive increase in chemical activity around the world, which was accompanied by a slew of destructive consequences for human health and the environment. The detection of dangerous compounds released into the environment in solid, liquid, and vapour forms has become critical in order to avoid the harmful impacts of these substances. Nanoscaled devices are required for biological applications to detect these hazardous substances. Discovery of suitable materials and their use in the construction of nanosensors that have low power consumption, great sensitivity, selectivity, and stability down to the level of

single molecules is thus a critical challenge. In this sector, silicene, a two-dimensional monolayer allotrope of silicon, is extremely important. The buckled structure of silicene helps to provide a one-of-a-kind feature that can be used in a variety of industries today. When compared to graphene, this buckling structure possesses essential features that allow the band gap of silicene to be adjusted more extensively.

Walia and Randhawa (2018) studied that silicene is a semimetal since it has no band gap. In addition, compared to a material with an intrinsic band gap, materials that are absent of bandgap do possess a small effect on the electronic characteristics due to adsorption of gas molecules. As a result, a band gap is necessary, which can be created using a variety of techniques. A lot of research on the adsorption characteristics of various materials on silicene have been conducted.

The adsorption of NH_3, NO, and NO_2 on silicene has been studied, and high adsorption energies have been reported (Fernández-Escamilla et al., 2019). P-type doping can be seen in the electronic properties of the resultant systems (Feng et al., 2014). Adsorption of other molecules on silicene has also been studied theoretically. Some of the molecules are CO, O_2, CO_2, and SO_2. However, due to its poor desorption rates once they are trapped, silicene cannot be used as a sensor for NO_2, O_2, or SO_2. For NO and NH_3, on the other hand, adsorption energies are smaller, allowing for easier desorption. Weak physisorption is used to absorb CO and CO_2. The surface of silicene reactivity is increased by mono-, di-, and tri-vacancies, as well as stone-wales defects. It is possible to detect hazardous compounds in this approach (Fernández-Escamilla et al., 2019).

1.4 Problem statement

Silicene is a two-dimensional material that has a buckled honeycomb surface and offers unique properties such as high thermal conductivity, greater chemical activity and has a Dirac cone where it is a surface that has special electron transport. Besides, silicene can also be used as a gas sensor due to its high surface area. Hence, understanding the effects of gas adsorption on silicene will help to know better the capabilities of it. In this research, we will look at the structural stabilities and also electronic properties of silicene with adsorbed CO gas molecules using DFT.

1.5 Objectives

The main objectives of this thesis are

1. To set up and utilize Quantum ESPRESSO for density functional theory (DFT) computation.
2. To analyse the electronic properties of the silicene structure with adsorbed gas molecules.
3. To determine the structural stabilities of a silicene structure system based on adsorption energy and bond length.

CHAPTER 2

LITERATURE REVIEW

A concise theoretical basis of properties of silicene, as well as the gas molecules adsorption on silicene, are discussed in this chapter. Density functional theory and Quantum ESPRESSO are also presented.

2.1 Properties of Silicene

Due to its potential compatibility with Si-based electronics, monolayer silicon (Si), generally known as silicene, has risen in popularity. Takeda and Shiraishi initially reported it in a theoretical research in 1994, then Guzman-Verri and Lew Yan Voon reinvestigated it in 2007, naming it silicene. Silicene is a two-dimensional sheet of hexagonally organised silicon atoms, similar to graphene but with out-of-plane buckling bonds (Roman & Cranford, 2014).

2.1.1 Structure of Silicene

There have been various theoretical research of structural characteristics published. Whether the local-density approximation (LDA) or the generalized-gradient approximation (GGA) to the exchange-correlation potential is used, first-principles calculations are always based on Density Functional Theory (DFT). In a DFT

computation, the atoms are relocated to reduce total energy while maintaining lattice symmetry (Spencer & Morishita, 2018).

In research from Lew (2015), Takeda and Shiraishi started by looking at the structure of a single Si layer. Figure 2.1 shows the crystal structure of silicene and sp^2 hybridization in silicon.

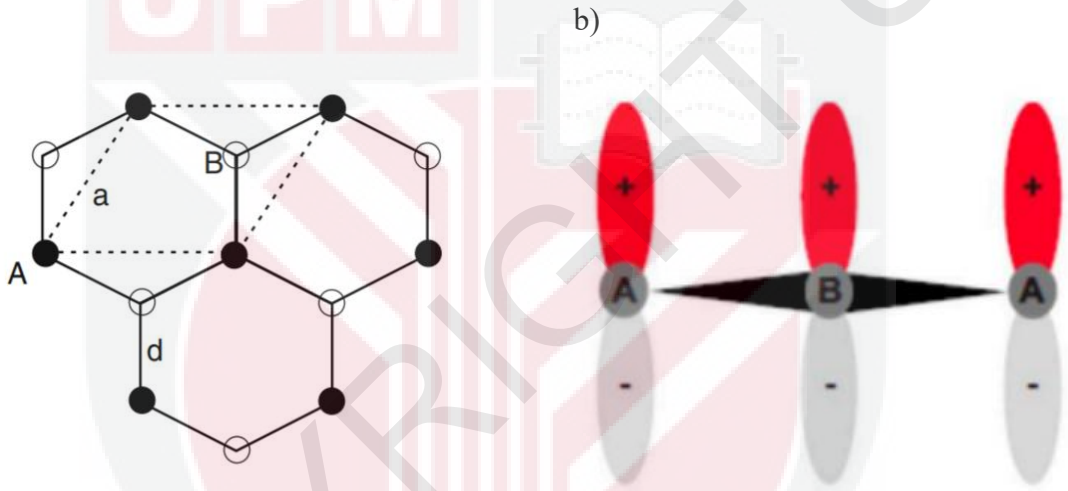

Figure 2.1: The visualization of a) crystal structure of silicene, the dashed lines indicate the unit cell and the basis is made up of two Si atoms, denoted by A and B, while b) the illustration of sp^2 hybridization in silicon (Chowdhury & Jana, 2016).

They discovered a local minimum at a = 3.855 Å and a deformation angle of 9.9 for the buckled structure, as well as a lower total energy than the flat one. According to a more current GGA estimate, the energy reduction is 30 meV/atom, with the binding energy of 4.9 eV/atom, which is 0.6 eV/atom lower than bulk silicon. The buckled structure strongly matches the bulk cubic silicon (111) plane (Kharadi et al., 2020). The weakening of the π double bond is due to the wider spacing of the Si atoms, and the

pseudo-Jahn–Teller effect with vibrational mode coupling of the electronic ground state to another, are two possible explanations for the buckled structure. (Yan Voon & Guzmán-Verri, 2014).

Table 2.1 shows typical structural parameters that are compared to a traditional molecular dynamics calculation. In research from Lew (2015), it mentioned that Cahangirov et al. calculated the out-of-plane height *z* of the Si atom to be 0.44 Å and Lew calculated it to be 0.45 Å. The out-of-plane Si atom in bulk Si is 0.78 Å from the (111) plane. As a result, the bonding in silicene can be thought of as being somewhere between sp^2 and sp^3. Due to the higher size of silicon compared to carbon, the bond length *d* is substantially longer if it were compared to graphene (Spencer and Morishita, 2018).

The low-buckled (LB) construction was found to be stable in a range of tests. When ab initio molecular dynamic (MD) was performed on a (4 × 4) supercell with a temperature of 1000 K, the LB structure was found to be retained. Additionally, the phonon spectrum has only positive frequencies. The lattice parameters are not correctly reproduced by standard MD computations. In another case, despite all of the DFT computations, a recent Monte Carlo simulation employing the Tersoff potential found no buckling (Kharadi et al., 2020).

Table 2.1: Structural parameters of silicene compared to graphene and germanene (Chowdhury & Jana, 2016).

Parameters	Graphene	Silicene	Germanene
Lattice constant a (Å)	2.468	3.858	4.06
Bond length d (Å)	1.424	2.232	2.341
Buckling parameter Δ_0 (Å)	0	0.42–0.45	0.69
Hopping integral t (eV)	2.8	1.6	1.3
Energy gap E_g (meV)	0.02	1.9	33
Fermi velocity $v_F(10^6\ ms^{-1})$	1.01	0.65	0.62
Effective electron mass $m^*(m_0)$	0	0.001	0.007
λ_{SO} (meV)	0.001	3.9	43
Rashba interaction (meV)	0.00	0.7	10.7
ΔE (eV)	8.7	7.2	8.1

The structural optimization described above considered a hexagonal cell, which is clearly a highly restrictive assumption. Other structures may have lesser energy, according to a more generic optimization. Lew (2015) also reported that Kaltsas and Tsetseris began by optimising the surface layer of several Si surface reconstructions by using different configurations. In this section, we will look at four common silicene structures that are currently being worked on, as illustrated in Figure 2.2. The first two are planar and simply buckled structures whereas the other two are based on recent experiments with (4×4) and $(\sqrt{3} \times \sqrt{3})$ structures.

(4 × 4) is labelled with regard to the Ag(111) surface lattice, while (√ 3×√ 3) is labelled with respect to the 1 × 1 silicene structure, as per experimental literature. The size of the unit cell and how the lattices are buckled are the key variations between these systems. The silicon atoms in the (√ 3×√ 3) structure in Figure 2.2(iii) are distributed across three horizontal planes, whereas those in the (4 × 4) structure in Figure 2.2(iv) are distributed across two horizontal planes (Spencer and Morishita, 2018). The simply buckled structure illustrated in Figure 2.2(ii) is the most stable form according to DFT, which is consistent with earlier findings (Huang et al., 2013).

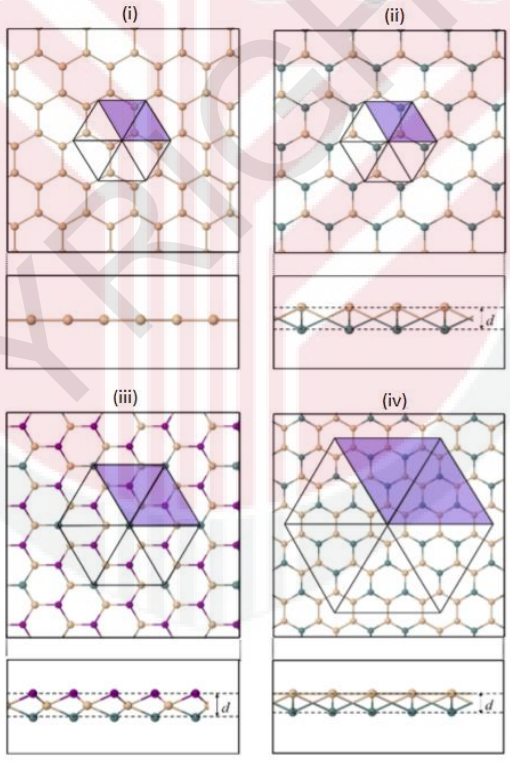

Figure 2.2: The visualization of (i) the planar silicene, (ii) simply buckled silicene, (iii) buckled silicene with a (√ 3×√ 3) unit cell and (iv) buckled silicene with a (4 × 4) unit cell. The buckling distance is denoted as *d*. Both top and side views are presented. Shadow regions presented the unit cells (Spencer & Morishita, 2018).

There are actually four possible adsorption sites on silicene, which are hill, valley, bridge and hollow. Usually, they are denoted as single alphabet such as B, V, H and T. Figure 2.3 shows the illustrations of the possible adsorption sites on silicene.

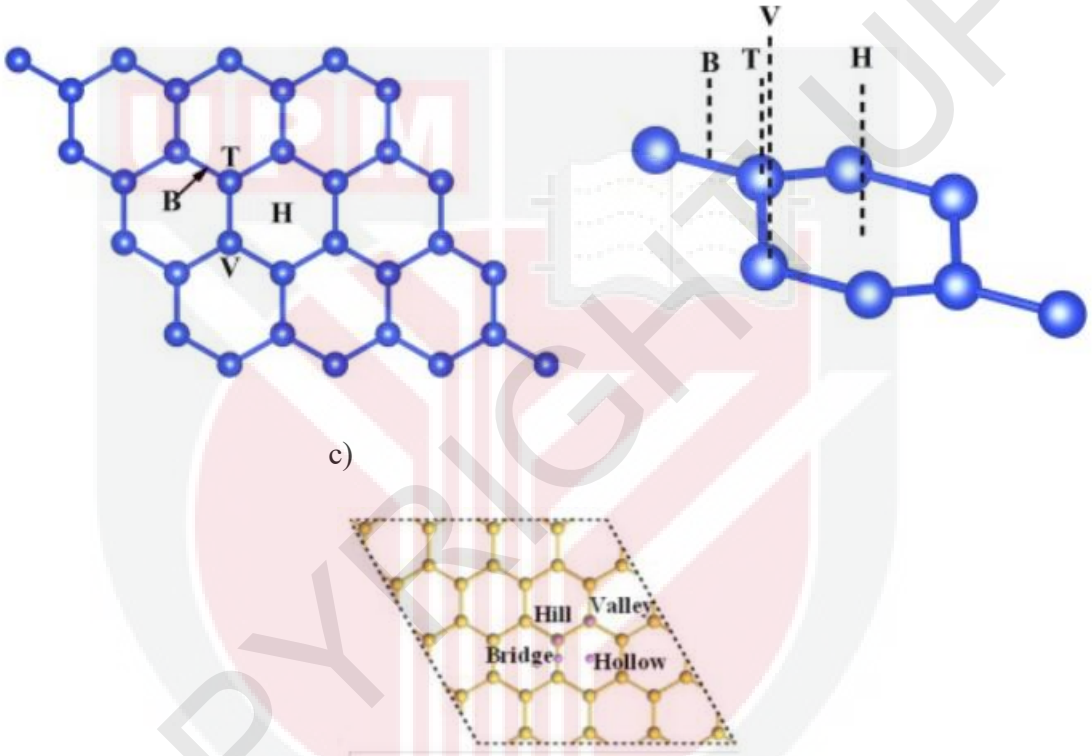

Figure 2.3: The illustrations of all possible adsorption sites on silicene.

2.1.2 Electronic Properties of Silicene

The existence of valence and conduction bands with linear dispersion, known as Dirac cones, crossing at the Fermi energy and at the K and K′ points in the hexagonal Brillouin zone has sparked researchers' curiosity in silicene and graphene (Lew, 2015). In the Brillouin zone, the Dirac cones form valleys, and the A and B sublattices of the

hexagonal structure, as shown in Figure 2.1(a), eventually lead to the two degenerate bands at any given position. These Dirac bands in graphene come from the pz states on each sublattice, which are dissociated from the other s and px, py states due to the graphene plane's reflection symmetry. The Hamiltonian in a tight-binding (TB) computation is of order two, and the Dirac bands were also linked to pseudospins (Kharadi et al., 2020).

Spencer and Morishita (2018) found that in a number of articles, the band structures of buckled and flat silicene have been examined. Spencer and Morishita also reported that while the past researchers, Lebègue and Eriksson (2009) compared silicene to planar Ge, other past researches like Suzuki and Yokomizo (2010) have made identical computations. Both types of silicene have been found to have electronic characteristics that are remarkably identical to graphene, including a zero π–π^* gap at the K point. While the Dirac cones have been detected in graphene, they are still an expectation for free-standing silicene, and whether they are present in silicene on silver remains a matter of debate, despite early claims of detection.

However, spin-orbit coupling was ignored in all of the computations above (Zhao et al., 2016). Adding the latter effect revealed that silicene would open a tiny gap of 1.55 meV. Figure 2.4 shows the band structures of graphene, silicene, and germanene (Lew, 2015).

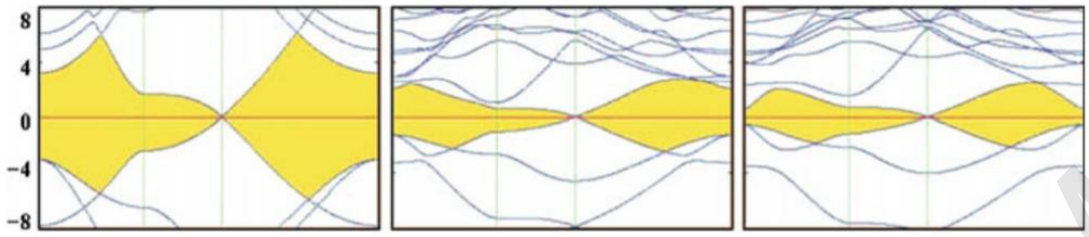

Figure 2.4: The illustration the band structures of graphene, silicene, and germanene, respectively (Lew, 2015).

2.2 Gas Molecules Adsorption On Silicene

Research from Spencer and Morishita (2018) shows that latest nanoscale physics research has focused on identifying new materials that have monolayer characteristic and showing their properties under various situations. When alternate atoms of hexagons are buckled, silicene was found to be the most stable of these materials.

Despite the fact that both theoretical and practical research show silicene to be stable, local imperfections can always occur at finite temperatures (Raya et al., 2021). Single foreign atoms can adsorb at flaw sites as a result of higher chemical activity among these (Spencer and Morishita, 2018). Dissociation of certain gas molecules into constituent atoms is possible. For the hydrogen economy, the dissociation of hydrogen, H, is extremely significant. When a nearly reversible oxidation–deoxidation mechanism contributing to a constant metal–insulator transition is possible, the oxidation of silicene preceded by the adsorption of O adatoms is of special interest (Raya et al., 2021).

The interaction of CO with silicene has also aroused attention in the development of gas sensors. These research are remarkable in this regard since they look at the interaction between different molecules and single vacancy sites. Theoretical research has also been done on the adsorption characteristics of atoms on silicene. However, due to its buckle structure, silicene has a far higher chemical reactivity for atom adsorption compared to graphene, making novel silicene-based nano-electronic devices ideal for many sectors such as industrial, environmental, and medicinal applications (Spencer and Morishita, 2018).

According to Feng et al. (2014), DFT was used to investigate the adsorption of many common gas molecules on silicene. The most stable configurations of many common gas molecules on silicene, as well as the accompanying adsorption energies, charge transfer, and electronic characteristics, are all thoroughly examined. We discovered that silicene has a strong reactivity towards some of the gas molecules, such as NO_2, O_2, and SO_2, with adsorption energies more than 1.00 eV, implying that it could be used in the creation of metal-free catalysts. Moreover, other gas molecules like NO and NH_3 were found to have reasonable adsorption energy of 0.35 eV and 0.60 eV respectively for their adsorption on silicene, implying that silicene could be an effective NO or NH_3 sensor.

Furthermore, adsorption of certain molecules except NO_2 in multiple ways opens the band gap of silicene, while NO_2 adsorption makes silicene half-metallic. They also discovered that the Stone–Wales defect and the Ag(111) substrate can boost chemical

reactivity of silicene. Their findings may be valuable not just in better understanding silicene's characteristics, but also in encouraging additional research into its potential applications in catalysis, gas detection, and electronics. The calculation of gas molecules adsorption on silicene-based material can be conducted using the following equation:

$$E_{ad} = E_{total} - [E_{silicene} + E_g] \quad (2.1)$$

where E_{ad} is the adsorption energy of gas molecule on silicene surface, E_{total} represents total energy of gas on silicene structure, $E_{silicene}$ is the total energy of silicene and E_g is the total energy of isolated gas (Wella et al., 2016). A higher E_{ad} value suggests stronger gas molecule adsorption on silicene in this definition.

The following Table 2.2 shows the adsorption energy (E_{ad}), charge transfer (δq), binding distance (d) and band gap (E_g) for the most stable configurations of two adsorbates on various silicene supercells. Figure 2.5 illustrates the most stable configuration for the two same adsorbates as mentioned in Table 2.2 (Feng et al., 2014).

Table 2.2: A table of adsorption energy (E_{ad}), charge transfer (δq), binding distance (d) and band gap (E_g) (Feng et al., 2014).

Silicene	E_{ad} (eV)	δq (e)	d (Å)	E_g (eV)
(a) CO				
4 × 4	0.71	−0.07	1.89	0.28
5 × 5	0.18	~0.00	4.02	~0.00
6 × 6	0.18	~0.00	4.04	~0.00
7 × 7	0.17	~0.00	4.04	~0.00
8 × 8	0.17	~0.00	4.04	~0.00
(b) NO				
4 × 4	1.22	−0.08	2.08	0.17
5 × 5	0.35	−0.08	2.10	0.08
6 × 6	0.35	−0.08	2.10	0.07
7 × 7	0.35	−0.08	2.10	0.05
8 × 8	0.35	−0.08	2.10	0.04

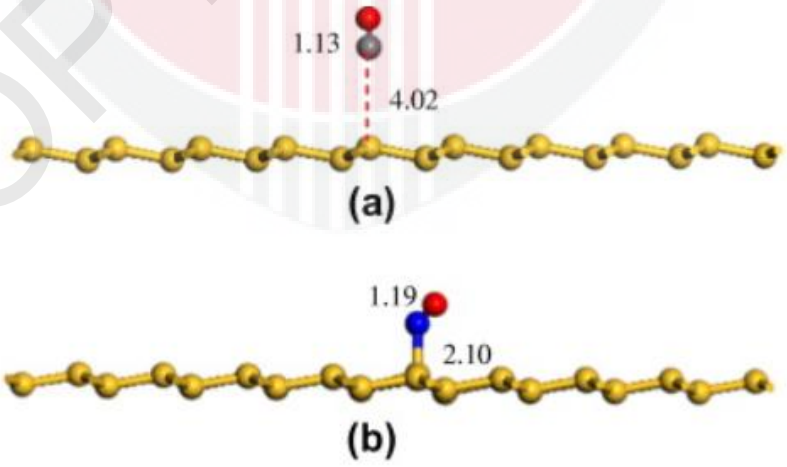

Figure 2.5: The illustration of the most stable configuration for the two same adsorbates as mentioned in Table 2.2, (a) C–Si distance is 4.02 Å while (b) the distance of the newly formed N–Si bond is 2.10 Å (Feng et al., 2014).

Studies on adsorption of gas molecules such as carbon monoxide, CO and nitric oxide, NO on silicene by using the first principles calculation are really popular and it shows that silicene is able to detect adsorbates and can act as a gas sensor.

2.3 Density Functional Theory

In research from Parr (1983), in a groundbreaking 1964 study by Hohenberg & Kohn, the density functional theory was born, and in a 1965 publication by Kohn & Sham, the main method of implementation was revealed. Despite this, the Annual Review of Physical Chemistry has only cited each of these studies once. Since its publication in the Annual Review of Physical Chemistry in 1983, the density-functional theory (DFT) of molecule electronic structure has been swiftly advancing (Parr and Yang, 1995).

Kohn et al. (1996) reported that DFT is basically an electronic ground state structure theory that is expressed in terms of the electronic density distribution $n(r)$. It has become much more helpful in understanding and calculating the ground state density, $n(r)$, and energy, E, of molecules, clusters, and solids of any system consisting of nuclei and electrons both with and without applied static alterations since its inception roughly three decades ago. It's a different and complementary technique to standard methodologies of quantum chemistry, which are based on the many-electron wave function $\Psi(r_1,...,r_N)$. Modern DFT may be traced back to the Thomas-Fermi and Hartree-Fock-Slater techniques. Modern DFT, on the other hand, is in principle precise, whereas those theories are basically estimations. DFT has become the tool of choice for physicists studying solid-state electronic systems over the last 30 years.

In research from Cataldo (2019), for solid state physics, DFT is by far the most prevalent quantum mechanical modelling method. The key reason for this is that it has a high degree of accuracy in comparison to its computational cost. All essential physical parameters can be written in terms of the electron density in DFT, as implied by its name.

Consider the electronic Hamiltonian in a solid inside the Born-Oppenheimer (BO) approximation to see why this is beneficial. We ignore the ion-ion interaction and ionic kinetic energy because we only worry about electrons.

$$H = -\sum_i \frac{\hbar^2 \nabla_i^2 m}{2} - \sum_{ij} \frac{Z_J e^2}{4\pi\epsilon_o |\vec{r}_i - \vec{R}_J|} + \frac{1}{2} \sum_{i \neq J} \frac{e^2}{4\pi\epsilon_o |\vec{r}_i - \vec{r}_j|} \quad (2.2)$$

where *r* denotes the position of electrons and *R* denotes the position of ions. The electronic kinetic energy, the ion-electron interaction and the electron-electron interaction are the three terms on the right hand side of the equations, respectively. It's important to mention here, as it will come up later, that we can think of the ion electron interaction as if the fixed ions provide an external potential that acts on the electrons.

We have first to solve Schrödinger's equation in order to express the N-electron system.

$$H\Psi = E\Psi \quad (2.3)$$

where Ψ represents the wavefunction of the N-electron system, and E represents its total energy. Hence, Ψ has to describe N electrons, with $N \approx 1023$, and every electron has 3 degrees of freedom, thus Ψ depends on $3N$ variables. Instead, if we describe the total energy E as a function of the electron density $n(\vec{r})$, we get $E = E[n(\vec{r})]$, where n is a three-variable function. This is possible, according to the first Hohenberg and Kohn theorem. The problem is not much easier to solve from an analytical standpoint because the explicit functional dependence of E on n is unknown, however it is a lot easier to solve numerically.

Specifically, for a constant number of electrons N, the electron density $n(\vec{r})$ that minimises $E[n]$ needs to be the ground state electron density of the N-electron system, according to the second Hohenberg and Kohn theorem. This means that we can start with any $n_o(\vec{r})$ and go through a minimization process until we reach a minimum of $E[n]$. The correct ground-state electron density will be n when E is minimised.

Up to this point, we have discovered that the total energy of the system can be described as a function of the electron density, and that the variational principle assures that we will be able to find a solution for the energy of the system, but we have no clue how to achieve it. The next move is to realize that the Hohenberg and Kohn theorems do not impose any constraints on the Hamiltonian of the system. In other words, they can be applied to a Hamiltonian with no electron-electron interaction.

This characteristic is exploited by Kohn and Sham, who come to a massive advantageous conclusion where it is workable to represent the ground state density $n(\vec{r})$ of the interacting N-electron system (with Hamiltonian) as the ground state density of a non-interacting system of N electrons in a fictitious external potential, called self-consistent potential (v_{scf}), formed in such a way that the correct ground state density is obtained. The reason why it is beneficial is because each time electrons are not interacting, we are able to decouple the Schrödinger's equation in N independent equations, in which is also called as Kohn & Sham equations, resolve them individually to acquire the single particle orbitals, which is also called as Kohn & Sham orbitals, and determine the ground state charge density from those.

$$\left\{-\frac{\hbar^2\nabla^2}{2m} + v_{scf}(\vec{r})\right\}\psi_i(\vec{r}) = \epsilon_i\psi_i(\vec{r}) \tag{2.4}$$

The ground state electron density can be obtained once the ψ are known by adding up the square modulus of the non-interacting Kohn & Sham ψ. In other words, $n(\vec{r}) = \sum_{i=1}^{N} |\psi_i(\vec{r})|^2$. Bear in mind that n is the same for interacting and non-interacting systems.

Starting with the ionic locations and the electron density $n(\vec{r})$, the form of $v_{scf}(\vec{r})$ can be generated using acceptable approximations on the dependency of the total energy on the electron density. It's worth noting that $n(\vec{r})$ is both a necessary component of the Hamiltonian and one of the results we're concerned about. The solution must be found using a self-consistent algorithm: we begin with a trial density $n_0(\vec{r})$, construct $v_{scf}(\vec{r})$,

solve, calculate $n_1(\vec{r})$, and so on, until our results remain consistent from one cycle to the next. The central loop in any DFT code is the self consistent (SCF) loop.

In short, we are able to calculate reliably the total energy of a given structure, band structure and density of states, forces acting on each atom, stress tensor, elastic properties, phonon frequencies, electric polarizability, Raman and Infrared activity, electron-phonon coupling and superconducting, *Tc*. Considering DFT is a ground-state theory, it is unable to calculate features that are time-dependent like excited states or responses to time-dependent fields.

2.4 Quantum ESPRESSO

In research from Giannozzi et al. (2020), Quantum ESPRESSO is a fully accessible application of computer codes for quantum-mechanical materials modelling based on density functional theory, pseudopotentials, and plane waves. It is commonly known for its work and conduction on a variety of hardware architectures, starting from laptops to enormously parallel computers, and also the breadth of its applications. They offer a concept and a short summary of the ongoing project to move Quantum ESPRESSO onto heterogeneous architectures based on hardware accelerators, which will eliminate the energy limits that are currently putting a stop to exascale computing.

Density-functional theory (DFT)-based numerical simulations have become a strong and frequently used technique for studying material characteristics. Various of these

simulations are based on the ‘plane-wave pseudopotential approach', in which they frequently use ultrasoft pseudopotentials or the projector augmented wave method (PAW), all of which will be referred to as ‘pseudopotentials'. Quantum ESPRESSO is a complete package of codes for electronic-structure computations that are based on DFT and utilising plane-wave basis sets and pseudopotentials, has played a compelling function in the diffusion of DFT-based approaches.

The main concept of Quantum ESPRESSO may be summed up in four words: openness, modularity, efficiency, and innovation. The distribution is built around two core packages, PWscf and CP, which perform self-consistent and molecular-dynamics calculations, respectively, as well as a number of other packages for more complex calculations. Some of the other packages that are required to solve more complex calculations are PHonon, for linear-response vibrational property calculations, PostProc which is responsible to postprocess and analyse data, XSpectra to solve the computation on absorption of x-ray and lastly GIPAW that is needed to solve the calculations of nuclear magnetic and electron paramagnetic resonance (Giannozzi et al., 2017).

In addition, Giannozzi et al. (2009) also studied that Quantum ESPRESSO employs a number of methodologies and algorithms targeted towards chemically realistic modelling of materials from the nanoscale upwards, utilizing a plane waves (PWs) basis set and pseudopotentials (PPs) to describe electron–ion interactions, and is based on the solution of the DFT issue. The following table, labelled as Table 2.3 shows the basic computations that can be performed.

Table 2.3: A summary of basic computations that can be performed.

No.	Type of computation	Notes
1.	Calculation of the Kohn–Sham (KS) orbitals and energies.	For isolated or extended systems and their ground-state energies.
2.	Complete structural optimizations of the microscopic and macroscopic degrees of freedom.	Utilization of Hellmann–Feynman forces and stresses.
3.	Ground state of magnetic or spin-polarized systems.	Includes spin-orbit coupling and non-collinear magnetism.
4.	Ab initio molecular dynamics, MD.	Applying either Car-Parrinello Langrangian or Hellmann-Feynman forces calculated on Born-Oppenheimer surface.
5.	Density Functional Theory, DFT.	To solve the computations of both second and third derivatives of total energy and any arbitrary wavelength other than preparing phonon dispersions, electron-phonon and phonon-phonon interactions and static response functions.
6.	Location of saddle points and transition states.	Via transition-path optimization using the nudged elastic band, NEB method.
7.	Ballistic conductance within Landauer-Büttiker theory.	Applying scattering method.

CHAPTER 3

METHODOLOGY

The setup of Quantum ESPRESSO, VESTA and other packages required to run density functional theory are covered in this chapter. The construction of a model of a unit cell is presented and the input file of quantum simulation is then described in detail. Apart from that, the procedure on how to obtain the kinetic energy cutoff, which is an important part of the calculation is also presented. The silicene sheet simulation and carbon monoxide (CO) adsorption on the silicene system are included in the last part.

3.1 Installation of Quantum ESPRESSO

Before we get to install Quantum ESPRESSO, we have to first prepare for our computational environment for our laptop PC. We can prepare it by using a virtual machine and following the need to install Ubuntu and a few other necessary packages. One of the available virtual machines is Virtual Box. The virtual machine for either Windows, Mac, Linux or Solaris is able to provide a perfect Ubuntu Linux environment, which is needed to run Quantum ESPRESSO. As the installation of Oracle VM Virtual Box and Ubuntu are required, hence the following essential procedures are followed.

We start by downloading Oracle VM VirtualBox at the main website, https://www.virtualbox.org/ with the available latest version provided. The installation of VirtualBox starts with clicking on the executable file (.exe) and proceeds to install the

program by following the required commands and instructions in the installation file. After we have finished installing the VirtualBox program, we have to execute the file. Then, we are required to set the information as follows:

Name: FYP Test

Type: Linux

Version: Ubuntu (64- bit)

After we have set the memory size as 5238 MegaByte, we need to create a virtual hard drive where it will help to allocate our hard disc memory.

Type: VirtualBox Disk Image

Size: 32 GigaByte

We continue with the installation of Ubuntu from the website http://www.ubuntu.com/ and download the latest version of Ubuntu Desktop. The downloaded files are utilised in order to boot up the system.

Before we can use Quantum ESPRESSO, some packages such as fftw3 and liblapack and fftw are required. We can install them by typing sudo apt-get install build-essential fftw3-dev gfortran and sudo apt-get install liblapack-dev fftw-dev. To download Quantum ESPRESSO, we can go to www.quantum-espresso.org. Once downloaded, we proceed with the following commands:

Type in tar xzvf espresso-6.1.tar.gz (follow the latest version that we have downloaded)

Type in cd espresso-6.1

Type in ./configure.

Type in make all

Type in gedit /.bashrc. (one file will be popping out after this command is typed in)

Add in export PATH=$PATH:/Users/Huawei/Desktop/espresso-6.7/bin/ at the end of file.

To install other software, we can use the following commands:

Type in sudo apt-get install xcrysden

Type in sudo apt-get install gnuplot

Other than Quantum ESPRESSO, there is another software that is essential for us to install and that is VESTA. VESTA stands for Visualization for Electronic and STructural Analysis and is a 3D visualization program for structural models, volumetric data such as electron or nuclear densities, and crystal morphologies (Momma, 2006). It can be downloaded from https://jp-minerals.org/vesta/en/download.html. Figure 3.1 shows the VESTA main interface.

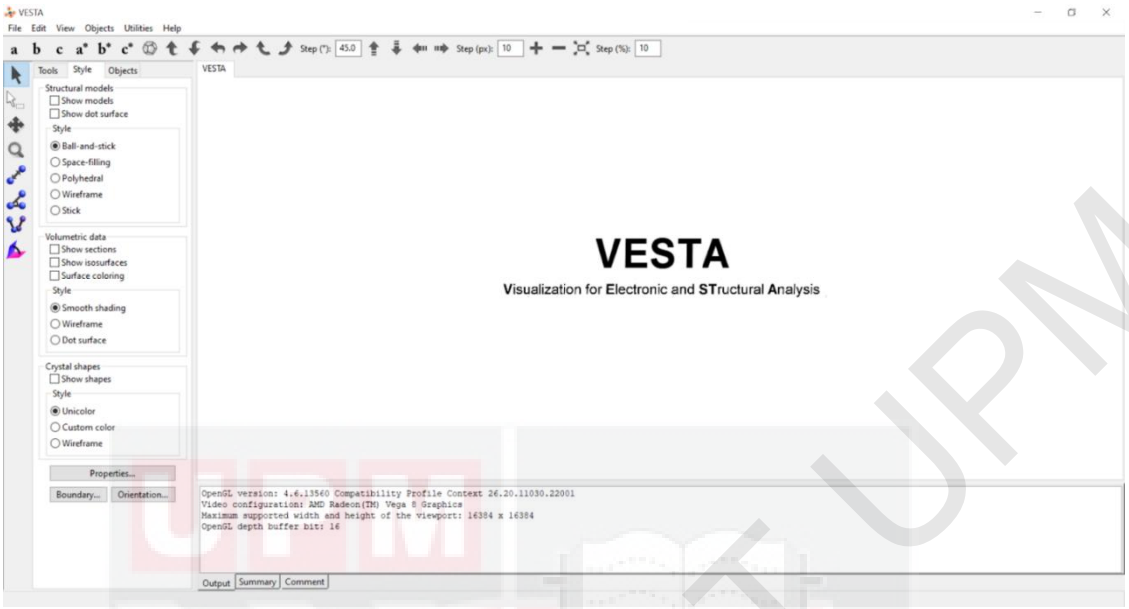

Figure 3.1: The main interface of VESTA

3.2 Material Modelling using VESTA

As mentioned before, VESTA is an application that helps to visualize structural models, volumetric data and crystal morphologies. Hence, it is required to help us in visualization of interatomic distances and bond angles.

3.2.1 Building unit cell using VESTA

Before we start to build our unit cell on VESTA, we need to prepare for the input file first. Input file of silicene is in CIF format and can be downloaded from the website https://materialsproject.org/materials/mp-165/. CIF stands for Crystallographic Information File. For monolayer silicene, it consists of two atoms. The CIF files can be

used by dragging it into VESTA software to build our unit cell. Now we can see the visualization of unit cell structure as shown in Figure 3.2.

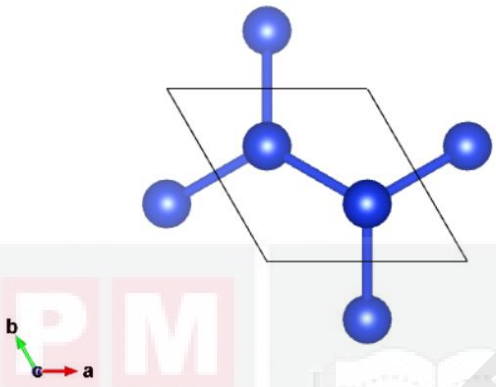

Figure 3.2: Visualization of unit cell structure

As mentioned in the previous paragraph, the unit cell of monolayer silicene must be two carbon atoms. Figure 3.3 shows that there are actually many carbon atoms in the cell due to the symmetry of the carbon. To make sure that we only have two carbon atoms, we then proceed to delete all those repeated unit cells by using tools that are available on the software.

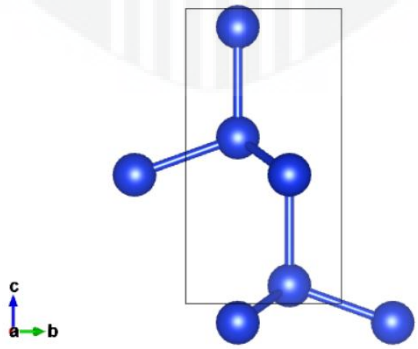

Figure 3.3: Illustration of the view along the a axis.

We are able to move the unit cell as shown above around by rotating and referring it to different axes. When we do the rotation according to the three different axes, we can easily delete all those repeated atoms. Hence, all the symmetry atoms are cancelled out and only two atoms are left behind. After all of the repeated carbon atoms are deleted, the file is exported or saved as VASP and XYZ files. Figure 3.4 shows the unit cell for silicene monolayer.

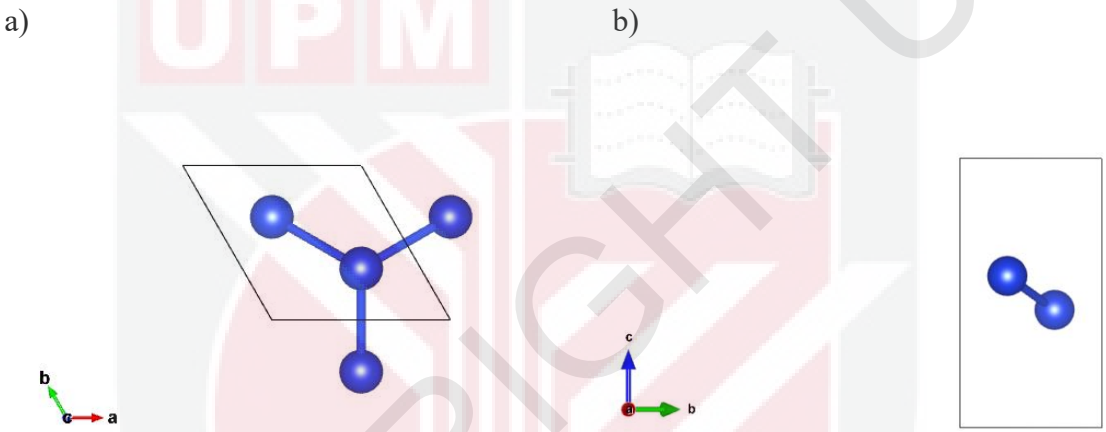

Figure 3.4: Visualization of unit cell for silicene monolayer a) with some symmetry atoms , while b) the exact unit cell with only two atoms.

3.2.2 Building Super Cell of Silicene

The building of a super cell (3 × 3) needs to start with alteration of the data in the unit cell and we are required to change it into a three times three (3 × 3) matrix by using the input file SiliceneMonolayer. After the transformation of a unit cell to a super cell, a VASP file is required to be exported and labelled as Silicene_3x3. Figure 3.5 illustrates the super cell.

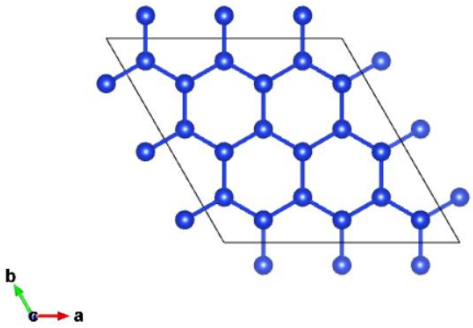

Figure 3.5: Illustration of silicene super cell.

Since this is a super cell, the total number of atoms now should be 2×3×3 which equals to 18 atoms. By using the same method and process in building the unit cell, all the repeated atoms are deleted. Figure 3.6 shows the complete 3 × 3 monolayer silicene.

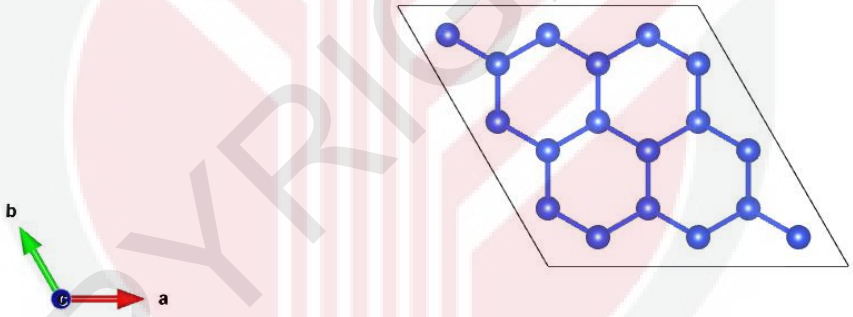

Figure 3.6: The visualization of complete 3 × 3 monolayer silicene.

3.2.3 Modelling CO Molecules

To model CO molecules, we first download its CIF files from https://materialsproject.org. Using back the same method as mention in Section 3.2.1, we manage to model the molecules in VESTA which is shown in Figure 3.7.

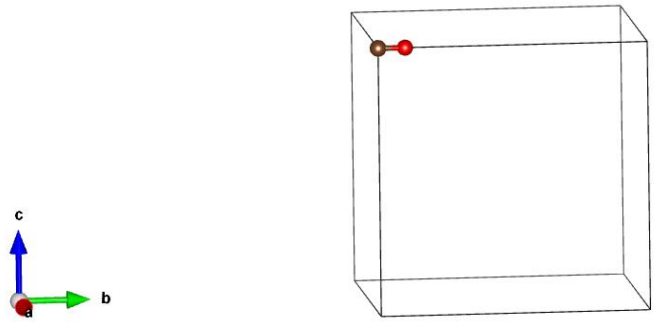

Figure 3.7: The visualization of CO molecule model.

3.2.4 Modelling of Adsorbed CO on Silicene

To model the gas molecule, carbon monoxide (CO) adsorbed on a 3 × 3 silicene, we adjusted VASP type of input file of Silicene_3x3. We include the CO molecule on silicene. Next, we add one carbon atom, C and one oxygen atom, O into the VASP file. Figure 3.8 illustrates the modelling of CO molecule in 3 × 3 silicene.

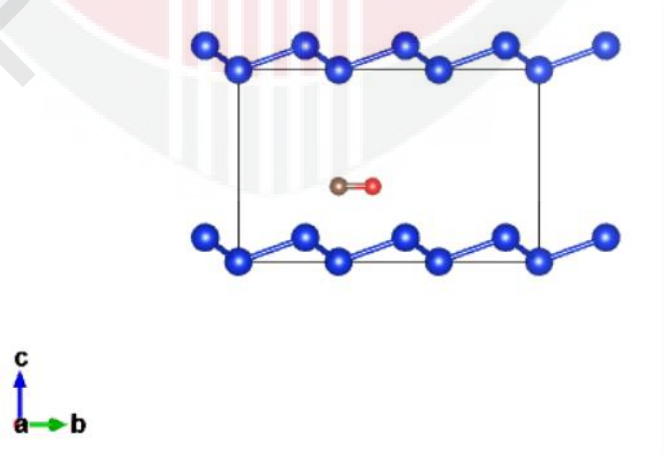

Figure 3.8: Illustration of modelling of CO molecules in 3 × 3 silicene.

Next, by using the same method as before, all of the repeated atoms are deleted. Hence, the model of adsorbed CO on 3 × 3 silicene is obtained.

3.3 Quantum Simulation on Silicene

Quantum simulation is crucial and has the potential to play big role in many different fields, including condensed matter physics, high-energy physics, atomic physics, quantum chemistry and cosmology. The simulation of properties of silicene can be performed using density function theory via Quantum ESPRESSO.

3.3.1 Input and Output File for QE Calculation

As we are using QE for our DFT calculation, we are required to prepare the input files that contain the essential information, coordinations and parameters for our calculation. One of the core packages for the calculation of electronic-structure properties within DFT, using a Plane-Wave (PW) basis set and pseudopotentials is PWscf, which stands for Plane-Wave Self-Consistent Field.

Before we can run the Quantum ESPRESSO, we will need the input file. The file contains the parameter needed to do the calculation. Figure 3.9 shows the input file for relax calculation while Figure 3.10 shows the input for scf calculation.

```
&CONTROL
    calculation='relax'
    prefix='silicene'
    restart_mode='from_scratch'
    outdir='./outdir'
    pseudo_dir='.'
    forc_conv_thr=1.0d-3  !Default
    etot_conv_thr=1.0d-4  !Default
    disk_io='none'  !Default is low
/
&SYSTEM
        ibrav = 4,
        a = 11.55145, !unit in A
        c = 15,    !unit in A
        nat = 18,
        ntyp = 1,
        ecutwfc = 40 ,
        ecutrho = 320 , !8 times ecut
        occupations = 'smearing', degauss = 0.01, smearing = 'gaussian',

/
&ELECTRONS
    conv_thr = 1.0d-6,  !Default
    mixing_beta = 0.7,  !Default value. 0.7 new 0.3 old files
/
&IONS
        ion_dynamics='bfgs' !Default for vc-relax and relax.
        ion_positions = 'from_input' , !This is not default

/
ATOMIC_SPECIES
Si 28.085 Si.pbe-nl-rrkjus_psl.1.0.0.UPF

ATOMIC_POSITIONS {angstrom}
Si     0.000000    0.000000    0.000000
Si    -1.925241    3.334615    0.000000
Si    -3.850483    6.669230    0.000000
Si     3.850482    0.000000    0.000000
Si     1.925241    3.334615    0.000000
Si    -0.000001    6.669230    0.000000
Si     7.700964    0.000000    0.000000
Si     5.775723    3.334615    0.000000
Si     3.850481    6.669230    0.000000
Si    -3.850483    8.892307    0.801510
Si    -0.000001    2.223078    0.801510
Si    -1.925242    5.557692    0.801510
Si    -0.000001    8.892307    0.801510
Si     3.850481    2.223078    0.801510
Si     1.925240    5.557692    0.801510
Si     3.850481    8.892307    0.801510
Si     7.700963    2.223078    0.801510
Si     5.775722    5.557692    0.801510

K_POINTS (automatic)
4 4 1 0 0 0
```

Figure 3.9: Relaxation calculation input file of silicene

```
&CONTROL
    calculation='scf'
    prefix='silicene'
    restart_mode='from_scratch'
    outdir='./outdir'
    pseudo_dir='.'
/
&SYSTEM
   ibrav = 4,
   a = 11.55145, !unit in A
   c = 15,    !unit in A
   nat = 18,
   ntyp = 1,
   ecutwfc = 70 ,
   ecutrho = 560 , !8 times ecut
   occupations = 'smearing', degauss = 0.01, smearing = 'gaussian',
   !nbnd =16,


/
&ELECTRONS
    conv_thr = 1.0d-6,
    mixing_beta = 0.7,
/
ATOMIC_SPECIES
Si 28.085 Si.pbe-nl-rrkjus_psl.1.0.0.UPF

ATOMIC_POSITIONS {angstrom}
Si     0.000000    0.000000    0.000000
Si    -1.925241    3.334615    0.000000
Si    -3.850483    6.669230    0.000000
Si     3.850482    0.000000    0.000000
Si     1.925241    3.334615    0.000000
Si    -0.000001    6.669230    0.000000
Si     7.700964    0.000000    0.000000
Si     5.775723    3.334615    0.000000
Si     3.850481    6.669230    0.000000
Si    -3.850483    8.892307    0.801510
Si    -0.000001    2.223078    0.801510
Si    -1.925242    5.557692    0.801510
Si    -0.000001    8.892307    0.801510
Si     3.850481    2.223078    0.801510
Si     1.925240    5.557692    0.801510
Si     3.850481    8.892307    0.801510
Si     7.700963    2.223078    0.801510
Si     5.775722    5.557692    0.801510

K_POINTS (automatic)
8 8 1 0 0 0
```

Figure 3.10: Self-Consistent Field calculation input file of silicene

The input file of PWscf is divided into two parts, those are NAMELISTS and INPUT CARDS. NAMELISTS are the standard input build in fortran90. There is a possibility for us to find the particular variables that are not necessary when we use NAMELISTS. We can also determine the sequence of the variables added. In the other hand, INPUT CARDS require data in specific order and are specific to Quantum ESPRESSO codes. We also need the input data provided by INPUT CARDS to specify the syntax used by NAMELISTS.

Three compulsory NAMELISTS in PWscf are &CONTROL, &SYSTEM and &ELECTRONS. The following is the brief explanation on each part. The first part is &CONTROL part. We need the software to run our calculations. The “from scratch” restart mode is selected. When the computation process finds a problem, this mode will cause it to restart automatically. The output file when the calculation is completed is called "outdir." The location of the file holding pseudopotential files is known as the "pseudo dir."

Next, the second part is &SYSTEM. “ibrav” is the setting of the crystal lattice type in the &SYSTEM section. The crystal perspective is represented by the numbering. For example, 1 denotes a simple cubic crystal structure and 2 denotes a face-centered cubic crystal structure. The length of the relevant lattice parameters for a, b, and c is shown by “celldm()”. The parameter c is only present because the system requires it; it will be set to an extremely big number to separate the layers. The unit for “celldm()” is Bohr radius. nat (each individual unique atom) specifies the number of atoms, while ntyp specifies

the number of different types of atoms (distinct chemistry). The Energy Cutoff in Rydbergs is ecutwfc. This is a crucial parameter to change when performing test.

&ELECTRONS, the "electrons" block, determines how the computation is carried out. To improve the charge density and wave functions towards the "true" solution, we use iterative diagonalization. conv_thr is the convergence threshold. When the energy changes by less than 10^{-8} Ryd every cycle, it is said to be self-consistent. This means that when the energy in each cycle changes by less than 10^{-8} Ryd, self-consistency is achieved. The diagonalization method is used to diagonalize the Kohn-Sham Hamiltonian. Davidson is doing great for the time being. The manner of mixing is referred to as the mixing mode. On the way to self-consistency, this dictates how the charge density is modified (mixed) from one stage to the next (Cataldo, 2019).

Apart from the three compulsory NAMELISTS in PWscf that have been mentioned above, there are another three NAMELISTS that need to be specified under certain conditions, &IONS, &CELL AND &EE. Firstly, &IONS are needed when atom moves, an input variables that control the ionic motion in molecular dynamics run or structural relaxation. Next, &CELL. This one is essential when cell moves. &CELL is an input variable that control the cell-shape evolution in a variable-cell-shape MD or structural relaxation. Lastly, &EE. This input variable is used to solve the problem with open boundary conditions and is required when density counter charge corrections.

In addition, there are also three essential INPUT CARDS, ATOMIC_SPECIES, ATOMIC_POSITIONS and K_POINTS. After the term ATOMIC_SPECIES, each ntyp has a line for "atomic-symbol," "atomic-weight," and "pseudo-potential." The pseudo-potential is the name of a file in pseudo dir after the keyword. A type of atomic position is ATOMIC_POSITIONS. For each nat, there is a line for the atomic-symbol x y z, with x, y, and z given in the units indicated by units, which can be alat, bohr, crystal, or angstrom. PWSCF is automatically told to construct a k-point grid when the keyword K_POINTS is used. The following line is nkx nky nkz offx offy offz in the case of automatic generation, where nk* is the number of intervals in a direction and off* is the offset of the grid's origin.

Quantum ESPRESSO currently supports pseudopotentials (PPs) in separable (Kleinman-Bylander) form. With the acknowledged tradeoff of designing and testing pseudopotentials that reproduce established benchmark structural and electrical properties, pseudopotential-based DFT allows for the determination of material properties with little computational effort (Rivero et al., 2015). As a consequence, many first-principles DFT codes, such as quantum ESPRESSO plane-wave basis sets, rely on the availability of high-quality pseudopotentials.

As a result, we will need a silicene pseudopotential file to complete the computation. We must perform various methods in order to obtain the pseudopotential file. To begin, go to http://www.quantum-espresso.org. We only need the silicon (Si) pseudopotential file, named as Si.pbe-n-kjpaw_psl.1.0.0.UPF file.

The lattice parameter changes depending on the crystal structure. In this case, the “ibrav” for silicene is 4 (hexagonal lattice). In the crystal structure, the letters "nat" stand for "number of atoms per unit cell" or "primitive cell." Since we wish to calculate on 3×3 silicene, the "nat" is 18. The number of different types of atoms in the structure is indicated by the “ntyp.” The “ntyp” equals 1 because we only use carbon for silicene. The “ecutwfc” indicates the energy cut-off for charge density and potential, whereas the “ecutrho” represents the kinetic energy cut-off. On the ELECTRONS card, there are only two important fields. The first is "conv the = 1.0d-6," which determines the energy of the convergence threshold of the final wave functions. When the self-consistent computation gives an energy difference of less than 10^8, the calculation is finished. When the system receives results, the field "mixing beta = 0.7" commands it to give them back with a percent equal to the "mixing beta" parameter.

3.3.2 Determination of the Kinetic Energy Cutoff and K-points

To determine the kinetic energy cutoff , we run the tests using input file and enter a number of kinetic energy cutoff in Quantum ESPRESSO to obtain the output. As a result, the data of total energy is our output. Ecut is set as 30, 35, 40, 45, 50, 55, 60, 65 and 70 in this project. All the total energy from the calculations will then be saved as etot_vs_ecut.data and after that we can plot the graph of “etot_vs_ecut.data” using gnuplot. From the plot, we can determine the best Ecut for later computation. It is important to have a stabilize Ecut value as this will optimize the computation particularly to save time and give out an accurate total ground state energy.

For K-points, before we run the scf calculation with variation of k-points mesh, specifically from value of 2 to 14, Ecut obtained from the previous convergence test is used in this calculation. Hence, we repeat the same process as in convergence test for Ecut and all total energy are saved in file etot_vs_kpoint.data. Graph is plotted to determine the best k-point mesh.

3.3.3 Relaxation, Self Consistent Field and Non-Self Consistent Field

After the convergence test is done, we can substitute the stabilize Ecut and best k-point values in the following input file to calculate the electronic properties of silicene. The input files are arranged in procedure as shown in Figure 3.13.

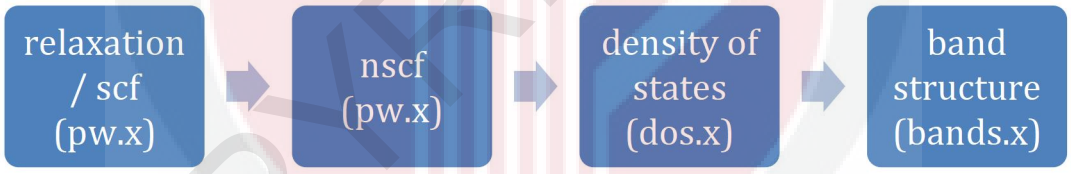

Figure 3.11: Calculation flow chart.

In order to run the calculation for relaxation, we must first key in our converged Ecut and k-point value here. The computation can be run by using pw.x and -np can also be used while running the calculation in parallel. The code to run Quantum Espresso (QE) pw.x is "~/Desktop/qe-6.8/bin/pw.x" and the code to run in parallel with four cores where it is divided into 2 pools is "mpirun -np 4 ~/Desktop/qe-6.8/bin/pw.x -npool 2 <input> output". The command needed to run calculations is shown in Figure 3.14.

```
&CONTROL
    calculation='relax'
    prefix='silicene'
    restart_mode='from_scratch'
    outdir='./outdir'
    pseudo_dir='.'
    forc_conv_thr=1.0d-3  !Default
    etot_conv_thr=1.0d-4  !Default
    disk_io='none'  !Default is low
```

Figure 3.12: The command for relaxation calculation.

The scf calculation is computed with the same procedure as relaxation calculation but the "calculation" part is changed to "calculation='scf' " instead, as shown in Figure 3.15. The optimize atomic position is copied from the output file of relaxation calculation and paste in the input file of scf calculation. Van der Waals correction is added into the scf input as well.

```
&CONTROL
    calculation='scf'
    prefix='silicene'
    restart_mode='from_scratch'
    outdir='./outdir'
    pseudo_dir='.'

&SYSTEM
   ibrav = 4,
   a = 11.55145, !unit in A
   c = 15,    !unit in A
   nat = 20,
   ntyp = 3,
   ecutwfc = 45 ,
   ecutrho = 360 , !8 times ecut
   occupations = 'smearing', degauss = 0.01, smearing = 'gaussian',
   vdw_corr = 'grimme-d2', !taking vdw interaction correction
```

Figure 3.13: The command of scf calculation.

The non-self consistent calculation in the other hand needs some alteration in the input file. Aside from the similar method with scf calculation, “nbnd” is added into nscf input file where “nbnd” is the number of bands per k-point. After making sure the prefix and the directory is same as in scf input file, we then must ensure that the value of nbnd follow the number of electron from scf output file. In addition, we also need to make sure that the value for k-point must be at least three times higher than the previous one in scf. The calculation is run by using pw.x and the code is the same as stated in relaxation part. We use tetrahedra method here for Density Of States (DOS) in which will be explained in the next sub-chapter with more details and step as this method is much faster. Figure 3.16 shows the input file of nscf calculation. Steps and procedure are repeated for adsorption of carbon monoxide (CO) on silicene. However, there are a few things that we must make sure to modify. First, the “nat” to be 20 as there are one carbon atom and one oxygen atom added into the system. The “ntyp” is changed to 3 as for three different types of atoms. Lastly, the pseudopotential files of carbon and oxygen are also added to the “ATOMIC_SPECIES” section.

```
 &CONTROL
                 calculation = 'nscf' ,
                restart_mode = 'from_scratch' ,
                      outdir = './outdir' ,
                  pseudo_dir = '.' ,
                      prefix = 'silicene' ,

 /
 &SYSTEM
   ibrav = 4,
   a = 11.55145, !unit in A
   c = 15,    !unit in A
   nat = 18,
   ntyp = 1,
   ecutwfc = 40 ,
   ecutrho = 320 , !8 times ecut
   nbnd = 51,
   occupations = 'tetrahedra',


 /
&ELECTRONS
    conv_thr = 1.0d-6,
    mixing_beta = 0.7,


 /
ATOMIC_SPECIES
Si 28.085 Si.pbe-nl-rrkjus_psl.1.0.0.UPF

ATOMIC_POSITIONS {angstrom}
Si            0.0000000000        0.0000000000        0.1664408287
Si           -1.9251964072        3.3345952403        0.1664860648
Si           -3.8504778160        6.6692784983        0.1664860648
Si            3.8504425912       -0.0000287387        0.1664860648
Si            1.9251964072        3.3345952403        0.1664860648
Si           -0.0000010000        6.6692300000        0.1664789531
Si            7.7010034088       -0.0000287387        0.1664860648
Si            5.7757230000        3.3346150000        0.1665199474
Si            3.8504758160        6.6692784983        0.1664860648
Si           -3.8505419236        8.8923410195        0.6350021734
Si           -0.0000010000        2.2230099609        0.6350021734
Si           -1.9252451452        5.5576901841        0.6350269207
Si           -0.0000010000        8.8923106317        0.6350269207
Si            3.8504498112        2.2230599931        0.6350488665
Si            1.9252431452        5.5576901841        0.6350269207
Si            3.8505399236        8.8923410195        0.6350021734
Si            7.7009941888        2.2230599931        0.6350488665
Si            5.7757220000        5.5577280138        0.6350488665

K_POINTS (automatic)
12 12 1 0 0 0
```

Figure 3.14: Input file of nscf calculation.

3.3.4 Computation of Ground State Energy

For the adsorption of carbon monoxide (CO) in silicene, we must first produce silicene sheet by using VESTA. The calculation of relaxation gives out output coordinate and it helps in the production of silicene sheet. Then, supercell is produced by editing the data and file is saved as VASP file.

The silicene sheet is then inserted with carbon and oxygen atoms. The position and distance of carbon monoxide atom is varied at four different adsorption sites which are hollow, bridge, site A and site B. The two sites, site A and site B are due to the buckled structure of silicene and site B is the buckled atom. These positions can be varied by altering the coordinates of atoms in input file. The distance between the position to place CO on silicene (3×3) sheet is fixed at 2.5 Å. The distance between carbon and oxygen atom is set at 1.128 Å. Figure 3.17 shows the altered coordinates of total 20 atoms for when silicene is adsorbed with CO at hollow site for first orientation. The step is repeated for three other sites with four orientations each. Therefore, there will be 16 orientations in total for adsorption of CO in silicene (3×3) sheet. Remember to ensure that all the units for atom coordinates are in Å. For the first and second orientations, carbon and oxygen atom are positioned side by side horizontally with carbon atom on the left side for first orientation and oxygen atom on the right side for second orientation. For third and fourth orientations, the two atoms are positioned side by side vertically with carbon atom on the upper side for third orientation and oxygen atom on the upper side for fourth orientation.

```
20
Si4
Si   -0.000000    2.223077    0.400758
Si   -1.925242    5.557692    0.400758
Si   -3.850483    8.892307    0.400758
Si    3.850482    2.223077    0.400758
Si    1.925240    5.557692    0.400758
Si   -0.000001    8.892307    0.400758
Si    7.700964    2.223077    0.400758
Si    5.775722    5.557692    0.400758
Si    3.850481    8.892307    0.400758
 C   -0.000001    6.669230    2.500000
 O   -0.000001    7.797230    2.500000
Si    1.925241    1.111538   -0.400758
Si    0.000000    4.446153   -0.400758
Si   -1.925242    7.780768   -0.400758
Si    5.775723    1.111538   -0.400758
Si    3.850482    4.446153   -0.400758
Si    1.925240    7.780768   -0.400758
Si    9.626206    1.111538   -0.400758
Si    7.700964    4.446153   -0.400758
Si    5.775722    7.780768   -0.400758
```

Figure 3.15: Coordinates when silicene is adsorbed with CO

3.3.5 Density Of States Calculation

After the calculation of nscf is done, we can run the input file of Density Of States (DOS) by using dos.x. The calculation can be used in parallel but not with npool. The code to run Quantum Espresso (QE) dos.x is “mpirun -np 4 ~/Desktop/qe-6.8/bin/dos.x <input> output”. Figure 3.18 shows the command for DOS input file.

```
 &DOS
prefix = 'silicene' ,
outdir = './outdir' ,
fildos = 'Si3x3.dos.dat' ,
```

Figure 3.16: The command for DOS input file.

The visualization of DOS file can be plotted using pDOSPlotting.gnu. Figure 3.19 shows the steps to be done in Gnuplot. The "xr" is the command that aids to fix the parameter of the graph and the command "[-7 : 3]" is the ratio setting for the graph.

```
# Gnuplot script file for plotting data in file "filename.dat"
set autoscale
unset log
set xtics 2
set title "Density of State for 3x3 Silicene"
set linetype 1 lc rgb "black" lw 1 pt 4  #pt is point type
set linetype 2 lc rgb "red" lw 2 pt 4 dt 3  #lw is line width
set linetype 3 lc rgb "green" lw 2 pt 4 dt 3  #lw is line width
set linetype 4 lc rgb "blue" lw 1 pt 4  #lw is line width

set xr [-7:3]
set ytic auto
#set ytics nomirror
#set y2tics
set xlabel "Energy (eV)"
set ylabel "Total and Partial Density of State (1/eV)"
#set y2label "Integrated density of states"
set key top right
set arrow 1 from 0, 0 to 0, 30 nohead ls 10 dt 2 #fermienergy
plot    "Si3x3.pdos.dat.pdos_tot" using ($1+2.300):2 with lines title "Silicene DOS" lt 1,\
        "pdos.s.dat" using ($1+2.300):2 with lines title "Silicene s orbital" lt 2,\
        "pdos.p.dat" using ($1+2.300):2 with lines title "Silicene p orbital" lt 3,\
```

Figure 3.17: The commands for DOS plotting in Gnuplot.

However, it is always nice to plot the partial DOS (pDOS) as well. This actually shows the contribution of all the orbital towards the density of states namely orbital s,p and d. In order to run the input file of pDOS, QE projwfc.x is used and the calculation cannot be run in parallel mode. Figure 3.20 shows the command for pDOS input file. Once this is performed, a lot of wave files will be produced. Therefore, we need to add them altogether. To add them, the following command must be used and steps are repeated for adsorption of CO on silicene:

1. To sum all the pDOS, the code to run is

~/Desktop/IntelQE6.5/bin/sumpdos.x *\(C\)* > "filename".dat

2. To sum s orbital, the code to run is

~/Desktop/IntelQE6.5/bin/sumpdos.x *\(C\)*\(s\) > “filename”.dat

3. To sum p orbital, the code to run is

~/Desktop/IntelQE6.5/bin/sumpdos.x *\(C\)*\(p\) > “filename”.dat

```
 &projwfc
prefix = 'silicene' ,
outdir = './outdir' ,
filpdos = 'Si3x3.pdos.dat' ,
```

Figure 3.18: The command for pDOS input file.

3.3.6 Band Structure Calculation

In order to run the band structure calculation, we first run the input file of scf again as it only takes few minutes to be completed. Then, we run the input file of bands using QE pw.x. In preparation to produce the input file of bands, the prefix and directory must be looked out as they are crucial parts and the k-points is a bit different here as we are using high symmetry point. The k-point values used can be referred to the values searched from the internet. However, we can always modify the order of symmetry point in order to get the results according to how we want it to be. Figure 3.21 shows the input file of bands. Once the calculation of bands is completed, we can continue to run the input file of band_pp using QE band.x. The computation can be done in parallel mode and after the calculation finished, we use run.py to plot the graph. Steps and

procedure are repeated for adsorption of CO on silicene. Figure 3.22 shows the command for bands_pp input file and Figure 3.23 shows the input file of run.py.

```
&CONTROL
    calculation = 'bands',
    prefix = 'silicene',
    restart_mode = 'from_scratch',
    outdir = './outdir',
    pseudo_dir = '.',
/
&SYSTEM
   ibrav = 4,
   a = 11.55145, !unit in A
   c = 15,    !unit in A
   nat = 18,
   ntyp = 1,
   ecutwfc = 40 ,
   ecutrho = 320 , !8 times ecut
   vdw_corr = 'grimme-d2', !taking vdw interaction correction
   nbnd = 51,

/
&ELECTRONS
    conv_thr = 1.0d-6,
    mixing_beta = 0.7,

/
ATOMIC_SPECIES
Si 28.085 Si.pbe-nl-rrkjus_psl.1.0.0.UPF

ATOMIC_POSITIONS {angstrom}
Si            0.0000000000        0.0000000000        0.1664408287
Si           -1.9251964072        3.3345952403        0.1664860648
Si           -3.8504778160        6.6692784983        0.1664860648
Si            3.8504425912       -0.0000287387        0.1664860648
Si            1.9251964072        3.3345952403        0.1664860648
Si           -0.0000010000        6.6692300000        0.1664789531
Si            7.7010034088       -0.0000287387        0.1664860648
Si            5.7757230000        3.3346150000        0.1665199474
Si            3.8504758160        6.6692784983        0.1664860648
Si           -3.8505419236        8.8923410195        0.6350021734
Si           -0.0000010000        2.2230099609        0.6350021734
Si           -1.9252451452        5.5576901841        0.6350269207
Si           -0.0000010000        8.8923106317        0.6350269207
Si            3.8504498112        2.2230599931        0.6350488665
Si            1.9252431452        5.5576901841        0.6350269207
Si            3.8505399236        8.8923410195        0.6350021734
Si            7.7009941888        2.2230599931        0.6350488665
Si            5.7757220000        5.5577280138        0.6350488665

K_POINTS (crystal_b)
4
0.3333333333    0.3333333333    0.0000000000 20 !K
0.0000000000    0.0000000000    0.0000000000 20 !Gamma
0.5000000000    0.0000000000    0.0000000000 20 !M
0.3333333333    0.3333333333    0.0000000000 20 !K
```

Figure 3.19: The input file of bands.

```
&bands  !use band.x
outdir = './outdir'
prefix = 'silicene'
filband = 'Si.bands.dat'
/
```

Figure 3.20: The command for bands_pp input file.

```
#!/usr/bin/env python
from Bands import *

datafile='Si.bands.dat.gnu'
fermi = -2.3
symmetryfile='6_Si_bands_pp.out'
bool_shift_efermi= True
fig, ax = plt.subplots()

#bndplot(datafile,fermi,symmetryfile,ax)
bndplot(datafile,fermi,symmetryfile,ax,shift_fermi=1,\
color='black',linestyle='solid',name_k_points=['K','G','M','K'],range=[-3,3])


fig.savefig("Si3x3.png")
plt.show()
```

Figure 3.21: The input file of run.py.

CHAPTER 4

RESULTS AND DISCUSSION

Convergence test is performed for kinetic energy cutoff and k-points and are presented in this chapter. These variables are needed to get optimized computation. Hence, we performed relaxation, scf, nscf, DOS and bands of (3 × 3) pristine silicene sheet and CO adsorbed silicene sheet.

4.1 Silicene Sheet Modelling

The (3×3) silicene sheet has in total of 18 silicon atoms in it but after being adsorbed with CO, the whole system have 20 atoms in total as there is an addition of one carbon atom and one oxygen atom. As mentioned before in Chapter 3, the distance between the position to place the CO molecule on silicene sheet has been fixed at 2.5 Å while the distance between carbon atom and oxygen atom in the molecule is set at 1.128 Å. There are four adsorption sites which are hollow, bridge, site A and site B and each of these sites have four different orientations namely Orientation 1, Orientation 2, Orientation 3 and Orientation 4 accordingly. Therefore, there are actually 16 different orientations of CO adsorbed silicene altogether. The (3×3) pristine silicene sheet and CO adsorbed silicene sheet are shown as in Figure 4.1 and in the following figure, the blue spheres represent eighteen silicon atoms, brown sphere represents carbon atom and the red sphere represents oxygen atom.

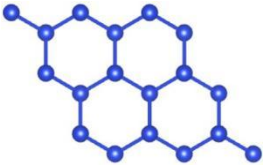

(a) Silicene

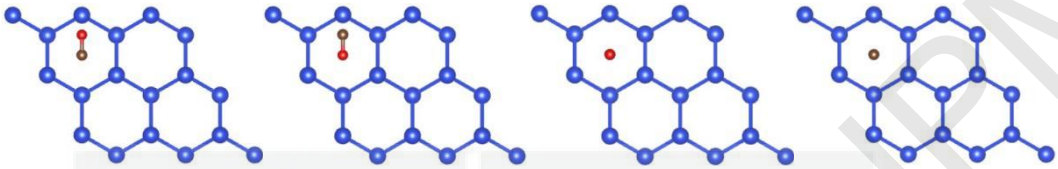

(b) Hollow site, from left to right are first to fourth orientation correspondingly

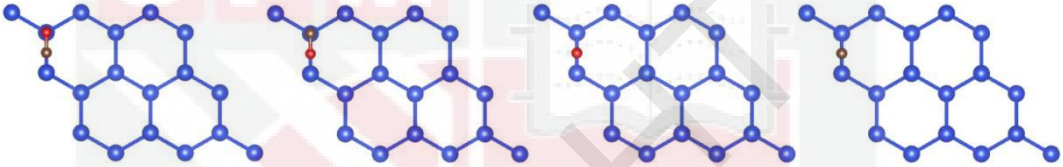

(c) Bridge site, from left to right are first to fourth orientation correspondingly

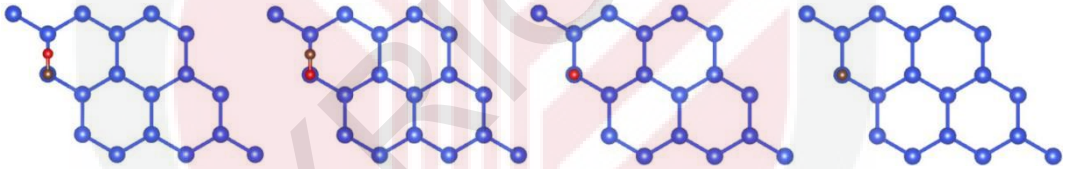

(d) Site A, from left to right are first to fourth orientation correspondingly

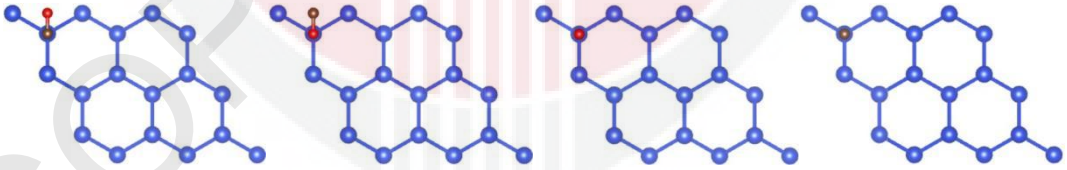

(e) Site B, from left to right are first to fourth orientation correspondingly

Figure 4.1: The (3×3) pristine silicene sheet and CO adsorbed silicene sheet.

4.2 Convergence Test of Kinetic Energy Cutoff and K-points

Convergence test is done to help us find the best values of kinetic energy cutoff and k-points. Silicene unit cell is the material used in the convergence test. After computing the input files of scf, ground state energy is obtained. Table 4.1 shows the convergence of total energy with respect to the kinetic energy cutoff and Figure 4.2 shows the graph of total energy versus kinetic energy cutoff. Next, Table 4.2 shows the convergence of total energy with respect to the k-points and Figure 4.3 shows the graph of total energy versus k-points. The optimize Ecut and k-point after convergence test are 50 Ry and 5 × 5 respectively.

Table 4.1: The convergence of total energy with respect to the kinetic energy cutoff where 1 Rydberg (Ry) is equals to 13.606 eV.

Kinetic Energy Cutoff (Ry)	Total Energy Cutoff (eV)	Difference (up to four decimal)
30	-182.68357008	0.0029
35	-182.68647834	0.0015
40	-182.68799901	0.0007
45	-182.68874335	0.0003
50	-182.68903567	0.0001
55	-182.68912521	0.0001
60	-182.68916008	0.0001
65	-182.68920934	0.0001
70	-182.68927196	Reference point

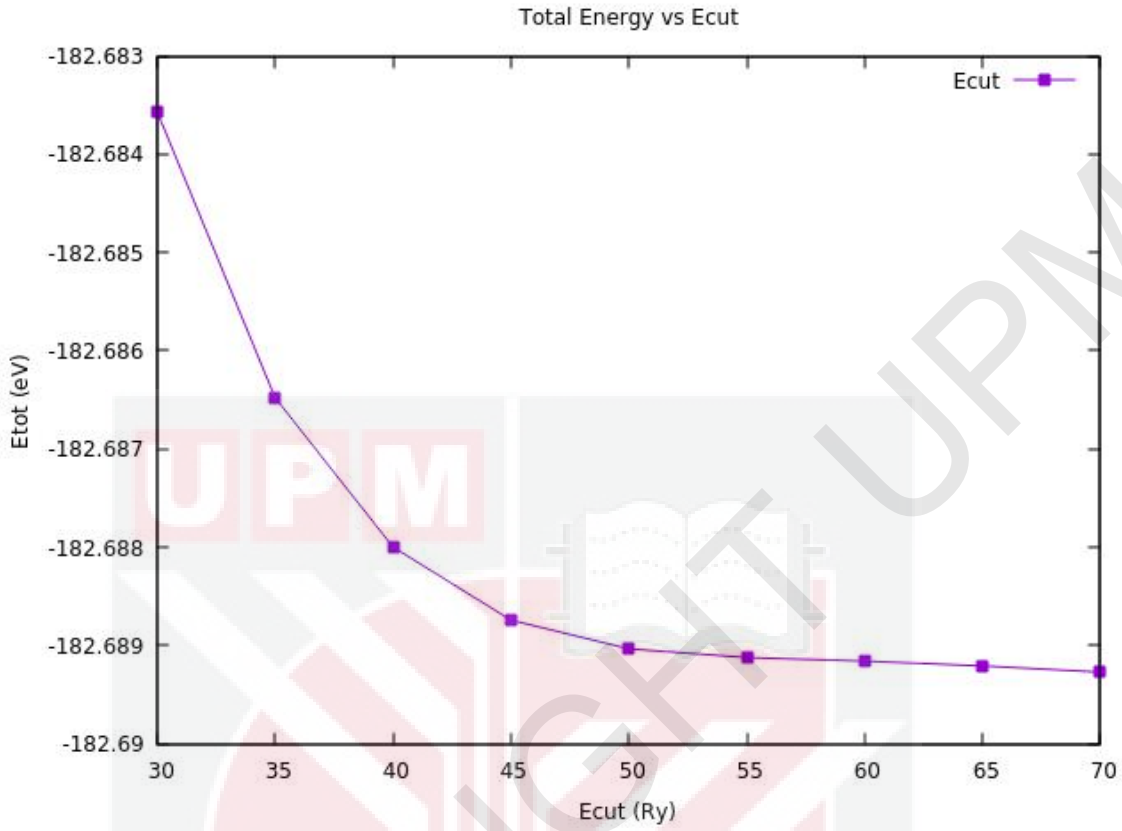

Figure 4.2: Graph of total energy versus kinetic energy cutoff.

Table 4.2: The convergence of total energy with respect to the k-points where 1 Rydberg (Ry) is equals to 13.606 eV.

K-points	Total Energy Cutoff (eV)	Difference (up to four decimal)
2 × 2 × 1	-182.97461306	0.0142
3 × 3 × 1	-182.98876574	0.0019
4 × 4 × 1	-182.99068792	0.0004
5 × 5 × 1	-182.99111010	0.0001
6 × 6 × 1	-182.99123628	0.0001
7 × 7 × 1	-182.99127713	0.0000
8 × 8 × 1	-182.99128947	0.0000
9 × 9 × 1	-182.99129239	0.0000
10 × 10 × 1	-182.99129327	Reference point

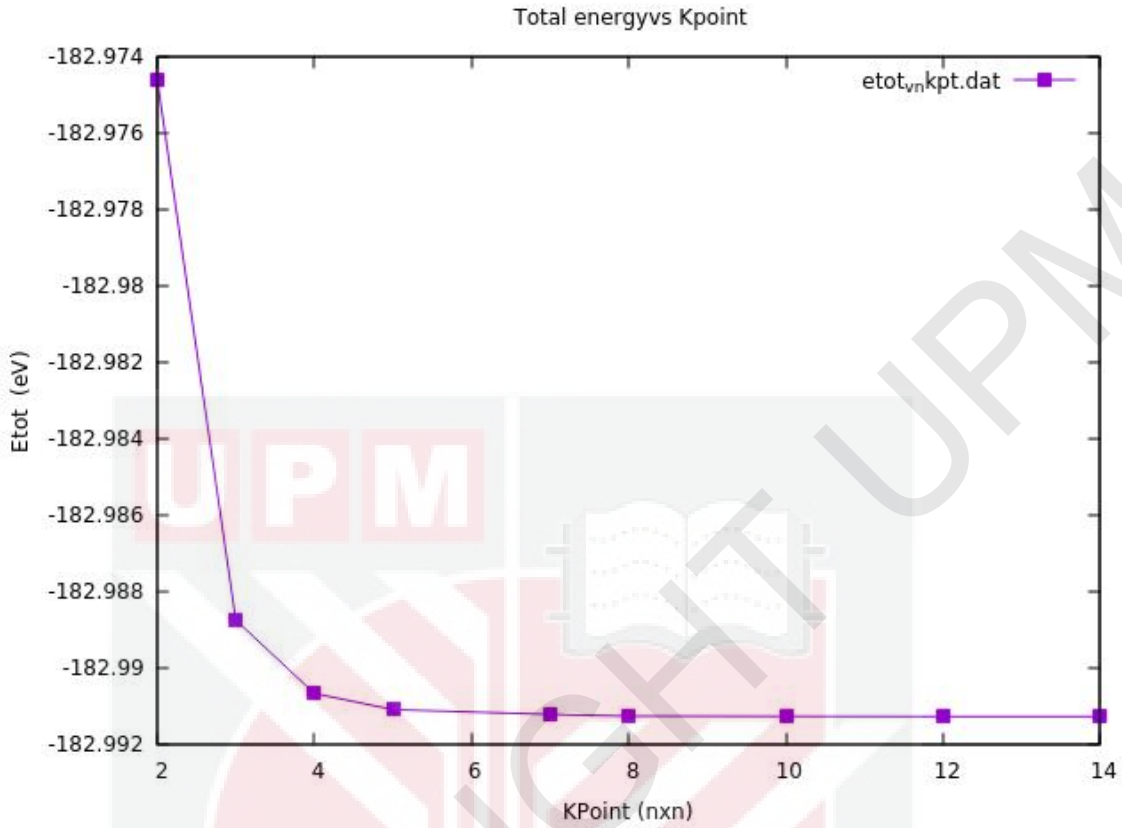

Figure 4.3: The graph of total energy versus k-points.

4.3 Structural and Electronic Properties of Silicene Sheet

The silicon-silicon bond length of pristine silicene sheet is found to be 2.36 Å. The discovered value is almost similar to the actual length of the normal bond which is 2.358 Å. In addition, the angle discovered between the silicon atoms are around 120° and it is very close to the angle of silicon atoms in actual silicene sheet which is 120°. The 120° shows that there is formation of sp^2 hybridization. The following Table 4.3 shows the tabulation of final output of simulation result with respect to the position of the silicon atom in silicene sheet.

Table 4.3: Final output of simulation result with respect to the position of the silicon atom in silicene sheet.

ID	Element	Position-x (crystal-primitive)	Position-y (crystal-primitive)	Position-z (crystal primitive)
1	Si	1.925239	1.111537	5.964928
2	Si	-0.000001	4.446149	5.964928
3	Si	-1.925246	7.780771	5.964928
4	Si	5.775729	1.111537	5.964928
5	Si	3.850489	4.446149	5.964928
6	Si	1.925244	7.780771	5.964928
7	Si	9.626207	1.111537	5.964928
8	Si	7.700967	4.446149	5.964928
9	Si	5.775722	7.780771	5.964928
10	Si	-0.000000	2.223074	6.766444
11	Si	3.850478	2.223074	6.766444
12	Si	-1.925246	5.557696	6.766444
13	Si	1.925233	5.557696	6.766444
14	Si	-3.850485	8.892308	6.766444
15	Si	0.000005	8.892308	6.766444
16	Si	7.700968	2.223074	6.766444
17	Si	5.775723	5.557696	6.766444
18	Si	3.850483	8.892308	6.766444

The following Figure 4.4 shows the density of states (DOS) and electronic band structure of pristine silicene sheet. DOS disclose the absence of states between valence bands and conduction. In addition, the absence of states explains the electronic structure of silicene as semi metallic as it possess zero band gap.

(a) DOS

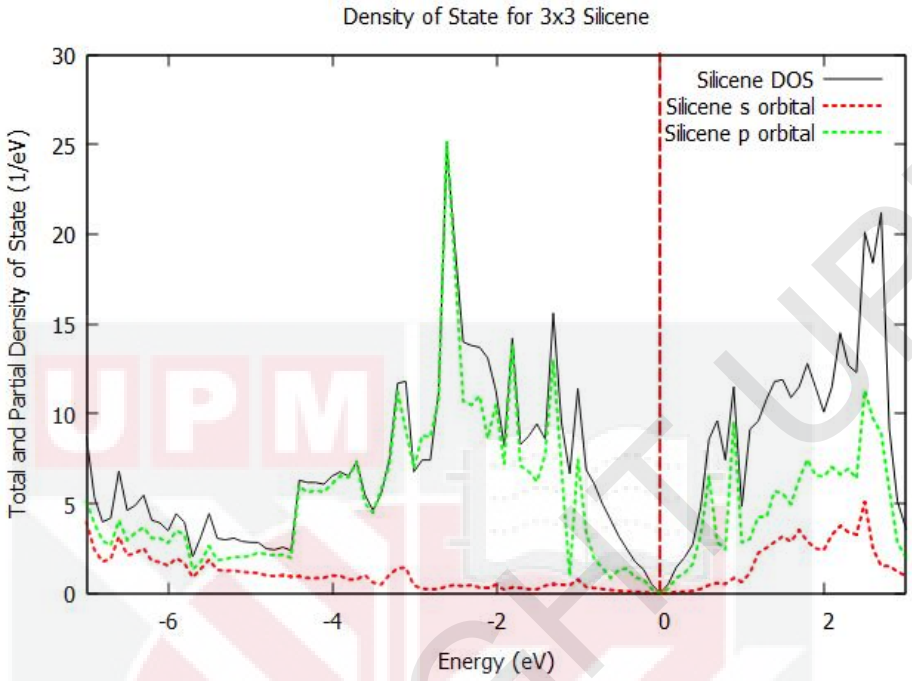

(b) Bands

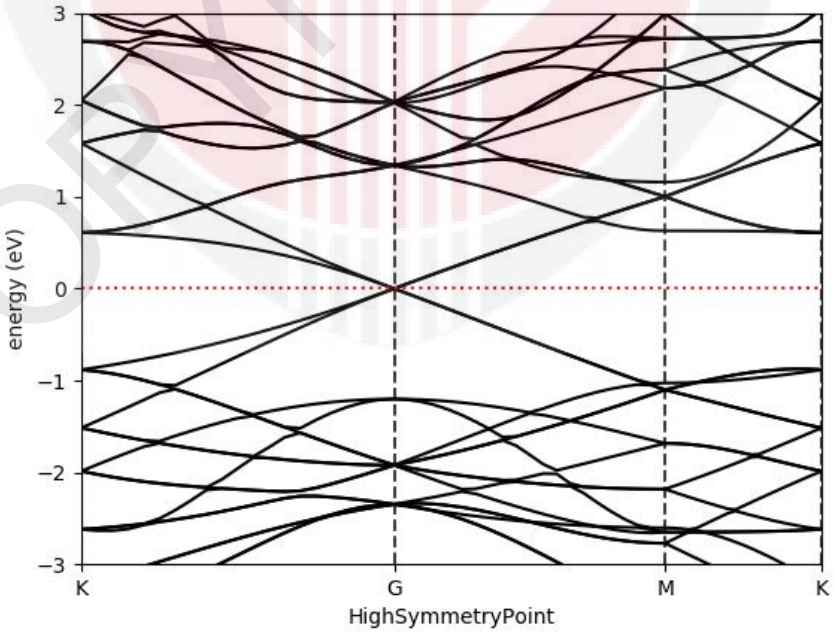

Figure 4.4: The density of states (DOS) and electronic band structure of pristine silicene sheet.

Based on the DOS and band structure of pristine silicene sheet above, we can see that pristine silicene sheet does not possess any band gap. From the DOS graph above, there are s and o orbital. There are actually four valence electrons in the outermost s and p orbitals electron configuration of silicene. Both of these two orbitals are not fully occupied and thus they are available for other interactions.

4.4 Structural Stabilities of CO on Silicene System

After relaxation calculation, CO is adsorbed on the silicene sheet. The relaxation computation is needed for the adsorption as the atomic coordinates that are obtained from it are used in scf calculation to acquire the ground state energy. The obtained energy is used to find the adsorption energy of CO on silicene sheet. Table 4.4 shows the result of relaxation output.

Table 4.4: The simulation output of CO adsorbed on silicene at four different sites with four different orientations each.

Site	Total energy (Ry)			
	Orientation 1	Orientation 2	Orientation 3	Orientation 4
Hollow	-228.610	-228.633	-228.651	-228.634
Bridge	-228.610	-228.590	-228.623	-228.604
Site A	-228.647	-228.647	-228.646	-228.646
Site B	-228.647	-228.647	-228.646	-228.646

From the data shown in Table 4.4, we can see that the CO/Silicene layer has the lowest total energy at the third orientation of hollow site. In this study, the absolute value was not taken into account. The lower the adsorption energy, the higher the stability of

adsorption. The adsorption energy is calculated using Equation (2.1). The obtained and calculated value of E_{ads} is -0.0902414251 eV / atom. Due to the small adsorption energy value, there is little interactions between CO and silicene monolayer. Therefore, CO is physisorbed on silicene via Van der Waals interactions.

After calculation of adsorption energy is done, the results follow the suggestion that has been made by the equation's conclusion such that lower ground state energy results in lower binding energy and thus the higher the stability of the adsorption.

4.5 Electronic Properties of Silicene Sheet Adsorbed with Carbon Monoxide

To gain the comprehension of the electronic properties of silicene adsorbed with CO, the following Figure 4.5 and Figure 4.6 show the DOS and electronic band structure of the adsorbed CO on silicene sheet.

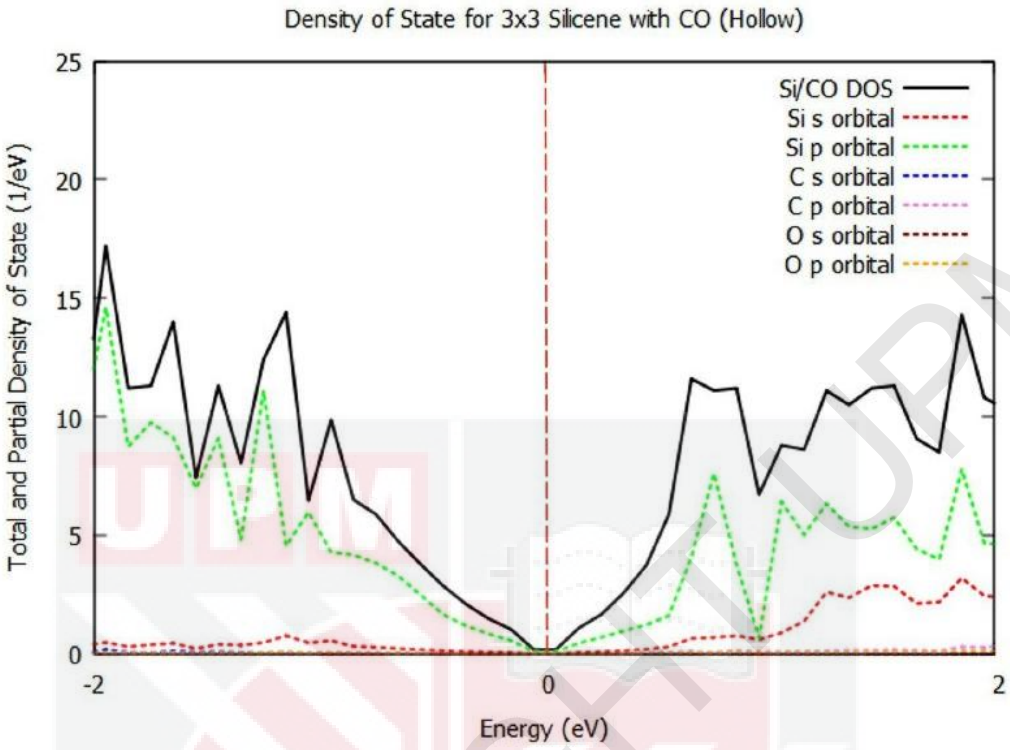

Figure 4.5: The density of state of adsorbed CO on silicene sheet

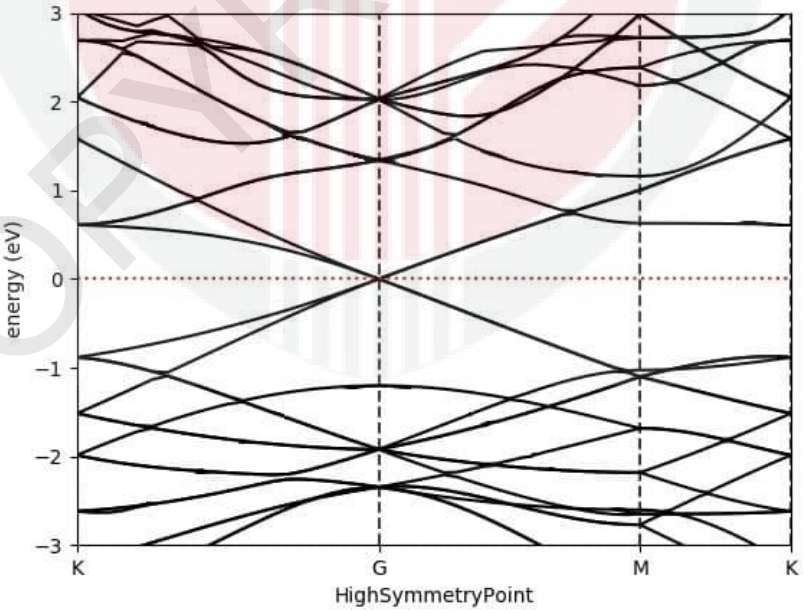

Figure 4.6: The electronic band structure of the adsorbed CO on silicene sheet

From the attached figures, we can see that adsorption of CO has made little alteration to the band structure. We can also see that pristine silicene sheet does possess band gap. This modification has shown that the band gap has been shifted and this indicates that our silicene monolayer is showing a potential semiconducting material.

CHAPTER 5

CONCLUSION

5.1 Conclusion

In this research, we have studied the first principle calculation for silicene system with adsorbed CO. We have successfully set up and utilized Quantum ESPRESSO for density functional theory computation. We also observed that the computational results are approximately similar to the theoretical values of adsorbed CO on silicene sheet. The structural stabilities of a silicene structure system has been determined based on adsorption energy and bond length.

Adsorption of CO on silicene system has shown to alter some structural and electronic properties. We discovered that the CO has the most stable configuration on the third orientation of hollow adsorption site due to the indication of lowest binding energy at the position and the calculated adsorption energy is -0.0902414251 eV / atom. From this study, it has been disclosed that one of the electronic properties is that the adsorption of CO does have an effect to the band gap of the silicene system where the band gap has been shifted as there is more gap to the band gap. These changes of electronic properties after the adsorption of CO onto silicene system presents a potential semiconductor material.

5.2 Future Works

From this research, the theoretical discussion of both structural and electronic properties of adsorbed CO on silicene sheet has been presented in details. However, there are a few suggestions and ideas that can be considered to investigate in future:

1. The adsorption onto the silicene sheet can be done with other toxic gasses and see if any of changes can be observed in the structural and electronic properties of silicene.
2. We can study another property that can be computed and studied which is magnetic properties such as finding magnetic impurities in silicene.

REFERENCES

Barea, E., Montoro, C., & Navarro, J. A. R. (2014). Toxic gas removal – metal–organic frameworks for the capture and degradation of toxic gases and vapours. *Chem. Soc. Rev.*, *43*(16), 5419–5430. https://doi.org/10.1039/c3cs60475f

Cataldo, S. (2019). *A quick introduction to Quantum Espresso*. Simone di Cataldo.

Dirac-cone Meaning | Best 1 Definitions of Dirac-cone. (2020). Your Dictionary. https://www.yourdictionary.com/dirac-cone

Drummond, N. D., Zólyomi, V., & Fal'ko, V. I. (2012). Electrically tunable band gap in silicene. Physical Review B, 85(7). https://doi.org/10.1103/physrevb.85.075423

Chowdhury, S., & Jana, D. (2016). A theoretical review on electronic, magnetic and optical properties of silicene. *Reports on Progress in Physics*, *79*(12), 1–6. https://doi.org/10.1088/0034-4885/79/12/126501

Critchley, L. M. (2018, April 13). *Electronic and Magnetic Properties of Silicene*. AZoM.Com. https://www.azom.com/article.aspx?ArticleID=15654

Feng, J. W., Liu, Y. J., Wang, H. X., Zhao, J. X., Cai, Q. H., & Wang, X. Z. (2014). Gas adsorption on silicene: A theoretical study. *Computational Materials Science*, *87*, 218–226. https://doi.org/10.1016/j.commatsci.2014.02.025

Fernández-Escamilla, H., Guerrero-Sánchez, J., Martínez-Guerra, E., & Takeuchi, N. (2019). Adsorption and dissociation of NO2 on silicene. *Applied Surface Science*, *498*, 143854. https://doi.org/10.1016/j.apsusc.2019.143854

Giannozzi, P., Andreussi, O., Brumme, T., Bunau, O., Buongiorno Nardelli, M., Calandra, M., Car, R., Cavazzoni, C., Ceresoli, D., Cococcioni, M., Colonna, N., Carnimeo, I., Dal Corso, A., de Gironcoli, S., Delugas, P., DiStasio, R. A., Ferretti, A., Floris, A., Fratesi, G., . . . Baroni, S. (2017). Advanced capabilities for materials modelling with Quantum ESPRESSO. *Journal of Physics: Condensed Matter*, *29*(46), 465901. https://doi.org/10.1088/1361-648x/aa8f79

Giannozzi, P., Baroni, S., Bonini, N., Calandra, M., Car, R., Cavazzoni, C., Ceresoli, D., Chiarotti, G. L., Cococcioni, M., Dabo, I., Dal Corso, A., de Gironcoli, S., Fabris, S., Fratesi, G., Gebauer, R., Gerstmann, U., Gougoussis, C., Kokalj, A., Lazzeri, M., . . . Wentzcovitch, R. M. (2009). QUANTUM ESPRESSO: a modular and open-source software project for quantum simulations of materials. *Journal of Physics: Condensed Matter*, *21*(39), 395502. https://doi.org/10.1088/0953-8984/21/39/395502

Giannozzi, P., Baseggio, O., Bonfà, P., Brunato, D., Car, R., Carnimeo, I., Cavazzoni, C., de Gironcoli, S., Delugas, P., Ferrari Ruffino, F., Ferretti, A., Marzari, N.,

Timrov, I., Urru, A., & Baroni, S. (2020). QuantumESPRESSO toward the exascale. *The Journal of Chemical Physics*, *152*(15), 154105. https://doi.org/10.1063/5.0005082

Huang, S., Kang, W., & Yang, L. (2013). Electronic structure and quasiparticle bandgap of silicene structures. *Applied Physics Letters*, *102*(13), 2–5. https://doi.org/10.1063/1.4801309

Jeevanandam, J., Barhoum, A., Chan, Y. S., Dufresne, A., & Danquah, M. K. (2018). Review on nanoparticles and nanostructured materials: history, sources, toxicity and regulations. *Beilstein Journal of Nanotechnology*, *9*, 1050–1074. https://doi.org/10.3762/bjnano.9.98

Kakaei, K., Esrafili, M. D., & Ehsani, A. (2019). Gas Convertor and Storage. *Interface Science and Technology*, *27*, 387–437. https://doi.org/10.1016/b978-0-12-814523-4.00010-1

Kharadi, M. A., Malik, G. F. A., Khanday, F. A., Shah, K. A., Mittal, S., & Kaushik, B. K. (2020). Review—Silicene: From Material to Device Applications. ECS Journal of Solid State Science and Technology, 9(11), 115031. https://doi.org/10.1149/2162-8777/abd09a

Kohn, W., Becke, A. D., & Parr, R. G. (1996). Density Functional Theory of Electronic Structure. *The Journal of Physical Chemistry*, *100*(31), 12974–12980. https://doi.org/10.1021/jp9606691

Lambrini, K., Christos, I., Petros, O., & Alexandros, M. (2018). Dangerous Gases and Poisoning: A Literature Review. *Journal of Healthcare Communications*, *03*(02). https://doi.org/10.4172/2472-1654.100136

Lew, L. Y. V. (2015). Electronic structure of silicene. Chinese Physics B, 24(8), 2–6. https://doi.org/10.1088/1674-1056/24/8/087309

Momma, K. (2006, November 27). *VESTA*. VESTA. https://jp-minerals.org/vesta/en/

Parr, R. G. (1983). Density Functional Theory. *Annual Review of Physical Chemistry*, *34*(1), 631–656. https://doi.org/10.1146/annurev.pc.34.100183.003215

Parr, R. G., & Yang, W. (1995). Density-Functional Theory of the Electronic Structure of Molecules. *Annual Review of Physical Chemistry*, *46*(1), 701–728. https://doi.org/10.1146/annurev.pc.46.100195.003413

Raya, S. S., Ansari, A. S., & Shong, B. (2021). Adsorption of gas molecules on graphene, silicene, and germanene: A comparative first-principles study. *Surfaces and Interfaces*, *24*, 101054. https://doi.org/10.1016/j.surfin.2021.101054

Roman, R. E., & Cranford, S. W. (2014). Mechanical properties of silicene. *Computational Materials Science*, *82*, 50–55. https://doi.org/10.1016/j.commatsci.2013.09.030

Rumbeiha, W. K., & Oehme, F. W. (2005). Veterinary Toxicology. *Encyclopedia of Toxicology*, 420–434. https://doi.org/10.1016/b0-12-369400-0/01004-8

Spencer, M., & Morishita, T. (2018). *Silicene: Structure, Properties and Applications (Springer Series in Materials Science, 235)* (Softcover reprint of the original 1st ed. 2016 ed., Vol. 235). Springer. https://doi.org/10.1007/978-3-319-28344-9

Walia, G. K., & Randhawa, D. K. K. (2018). Adsorption and dissociation of sulfur-based toxic gas molecules on silicene nanoribbons: a quest for high-performance gas sensors and catalysts. *Journal of Molecular Modeling*, *24*(4). https://doi.org/10.1007/s00894-018-3631-x

Wella, S. A., Syaputra, M., Wungu, T. D. K., & Suprijadi. (2016). The study of electronic structure and properties of silicene for gas sensor application. *The Study of Electronic Structure and Properties of Silicene for Gas Sensor Application*, *1719*(1), 1–5. https://doi.org/10.1063/1.4943734

Yan Voon, L. L., & Guzmán-Verri, G. (2014). Is silicene the next graphene? *MRS Bulletin*, *39*(4), 366–373. https://doi.org/10.1557/mrs.2014.60

Zhao, J., Liu, H., Yu, Z., Quhe, R., Zhou, S., Wang, Y., Liu, C. C., Zhong, H., Han, N., Lu, J., Yao, Y., & Wu, K. (2016). Rise of silicene: A competitive 2D material. *Progress in Materials Science*, *83*, 24–151. https://doi.org/10.1016/j.pmatsci.2016.04.001

Zhuang, J., Xu, X., Feng, H., Li, Z., Wang, X., & Du, Y. (2015). Honeycomb silicon: a review of silicene. *Science Bulletin*, *60*(18), 1551–1562. https://doi.org/10.1007/s11434-015-0880-2

APPENDICES

Example of Output File for Hollow Site (DOS)

```
Program DOS v.6.8 starts on 29Nov2021 at 12:26:29

This program is part of the open-source Quantum ESPRESSO suite
for quantum simulation of materials; please cite
    "P. Giannozzi et al., J. Phys.:Condens. Matter 21 395502 (2009);
    "P. Giannozzi et al., J. Phys.:Condens. Matter 29 465901 (2017);
    "P. Giannozzi et al., J. Chem. Phys. 152 154105 (2020);
     URL http://www.quantum-espresso.org",
in publications or presentations arising from this work. More details at
http://www.quantum-espresso.org/quote

Parallel version (MPI), running on     4 processors

MPI processes distributed on     1 nodes
R & G space division:  proc/nbgrp/npool/nimage =      4
7957 MiB available memory on the printing compute node when the environment starts


Reading xml data from directory:

./outdir/SiCOhollowori3.save/

IMPORTANT: XC functional enforced from input :
Exchange-correlation= PBE
                     (   1   4   3   4   0   0   0)
Any further DFT definition will be discarded
Please, verify this is what you really want


Parallelization info
--------------------
sticks:   dense  smooth     PW     G-vecs:    dense   smooth      PW
Min        2950    1480    388               337252   119316   16186
Max        2951    1481    389               337259   119319   16193
Sum       11803    5923   1555              1349025   477271   64761

Using Slab Decomposition


Check: negative core charge=   -0.000004

negative rho (up, down):  1.109E-03 0.000E+00

Tetrahedra used

DOS          :     12.14s CPU     14.52s WALL
```